cal Disease Activity Index) をはじめとする臨床的寛解基準を用いたとしても困難である。生物学的製剤有効例においても効果が減弱し関節破壊が進行する例が存在すること，骨びらんと異なり一度破壊された軟骨組織の修復は極めて困難であることを考慮すると，臨床的評価基準の他に，炎症とは独立した関節破壊進行を評価できる軟骨マーカーの存在意義は大きいと考えられる。

文　献

1) Emery P, Breedveld FC, Hall S, et al : Comparison of methotrexate monotherapy with a combination of methotrexate and etanercept in active, early, moderate to severe rheumatoid arthritis (COMET) : a randomised, double-blind, parallel treatment trial. Lancet **372** : 375-382, 2008.
2) Landewé R, van der Heijde D, Klareskog L, et al : Disconnect between inflammation and joint destruction after treatment with etanercept plus methotrexate : results from the trial of etanercept and methotrexate with radiographic and patient outcomes. Arthritis Rheum **54** : 3119-3125, 2006.
3) Garnero P, Piperno M, Gineyts E, et al : Cross sectional evaluation of biochemical markers of bone, cartilage, and synovial tissue metabolism in patients with knee osteoarthritis : relations with disease activity and joint damage. Ann Rheum Dis **60** : 619-626, 2001.
4) Lamers RJ, van Nesselroqij JH, Kraus VB, et al : Identification of an urinary metabolite profile associated with osteoarthritis. Osteoarthritis Cartilage **13** : 762-768, 2005.
5) Vignon E, Garnero P, Delmas P, et al : Respect of Ethics and Excellence in Science (GREES) : Osteoarthritis Section Recommendations for the registration of drugs used in the treatment of osteoarthritis : an update on biochemical markers. Osteoarthritis Cartilage **9** : 289-293, 2001.
6) 伊達秀樹，山田治基，森田充浩ほか：血清マーカーによる変形性関節症の病態評価，進行予知．別冊整形外科 **53** : 60-66, 2008.
7) Takeuchi T, Yamanaka H, Inoue E, et al : Retrospective clinical study on the notable efficacy and related factors of infliximab therapy in a rheumatoid arthritis management group in Japan : one-year outcome of joint destruction (RECONFIRM-2J). Mod Rheumatol **18** : 447-454, 2008.
8) Wakitani S, Nawata M, Kawaguchi A, et al : Serum keratan sulfate is a promising marker of early articular cartilage breakdown. Rheumatology (Oxford) **46** : 1652-1656, 2007.
9) van den Berg WB : Joint inflammation and cartilage destruction may occur uncoupled. Springer Semin Immunopathol **20** : 149-164, 1998.
10) Brown AK, Conaghan PG, Karim Z, et al : An explanation for the apparent dissociation between clinical remission and continued structural deterioration in rheumatoid arthritis. Arthritis Rheum **58** : 2958-2967, 2008.
11) Kong SY, Stabler TV, Criscione LG, et al : Diurnal variation of serum and urine biomarkers in patients with radiographic knee osteoarthritis. Arthritis Rheum **54** : 2496-2504, 2006.
12) Roos H, Dahlberg L, Hoerrner LA, et al : Markers of cartilage matrix metabolism in human joint fluid and serum : the effect of exercise. Osteoarthritis Cartilage **3** : 7-14, 1995.
13) Gordon CD, Stabler TV, Kraus VB : Variation in osteoarthritis biomarkers from activity not food consumption. Clin Chim Acta **398** : 21-26, 2008.

日整会誌 (J. Jpn. Orthop. Assoc.) 86：394-400 2012

シンポジウム　RA 生物学的製剤治療の最前線　—寛解を目指して—

生物製剤の登場による手術療法の動向と適応の変化について*

西田圭一郎[1]　中原龍一[2]　橋詰謙三[2]　斎藤太一[2]
金澤智子[2]　小澤正嗣[2]　那須義久[3]　尾﨑敏文[2]

生物学的製剤登場後の 8 年を振り返って

生物学的製剤の導入から 9 年目となり，積極的なメトトレキサート(methotrexate, MTX)の使用とともに，以前より増して関節リウマチ(rheumatoid arthritis, RA)の薬物コントロールが良好になされるようになってきた．生物学的製剤は，特に MTX との併用において，早い臨床効果の発現，短・中期的な関節破壊防止効果のエビデンスを有し[1)-5)]，さらには破壊された関節に対する修復反応も見られるようになって，早期に診断され，関節破壊を来す以前に至適な薬物治療により適切に疾患コントロールが得られれば，手術の回避はもちろん，一部の患者では寛解も夢ではなくなってきた．わが国より約 5 年早く生物学的製剤が導入された欧米において，2002 年の米国リウマチ学会の早期 RA に対する治療ガイドラインでは，薬物治療がいずれも無効の場合に外科的治療が位置づけられており，実際，ノルウェー，デンマーク，フィンランド，スウェーデンのレジストリーからは手術件数の減少，人工関節手術の減少が報告されている[6)-9)]．一方で，生物学的製剤による治療の問題点として，①生物学的製剤不応例や二次無効，②副作用で中止せざるを得ない場合，③経済的問題・合併症のため使用できない場合，④休薬や薬剤変更の間に関節破壊が進行する場合，⑤全身的に効果が認められるが一部の関節で炎症が持続する場合や関節破壊が進行する場合，⑥長期罹病患者ではすでに関節破壊や変形を来してこれが不可逆的になっている場合，などが次々と経験されるようになってきた．こういった背景のもとでは，従来どおり薬物治療に外科的治療やリハビリテーションを適切に組み合わせた治療戦略が必須である．われわれ整形外科医は新しい薬物治療の時代における「寛解とはなにか」を考えるにあたって，整形外科医がリウマチ診療に積極的に参加している本邦での外科的治療の動向と適応の変化を知ることは重要である．

Key words: Rheumatoid arthritis, Biologic DMARD, Orthopaedic surgery, Japanese treat to target (T2T)

*Trend and practice of orthopaedic surgery for rheumatoid arthritis in the era of biologic agents

[1]岡山大学大学院医歯薬学総合研究科人体構成学分野．Keiichiro Nishida: Department of Human Morphology, Okayama University Graduate School of Medicine, Dentistry and Pharmaceutical Sciences.
[2]岡山大学大学院医歯薬学総合研究科整形外科学．Ryuichi Nakahara, Kenzo Hashizume, Taichi Saito, Tomoko Kanazawa, Masatsugu Ozawa, Toshifumi Ozaki: Department of Orthopaedic Surgery, Okayama University Graduate School of Medicine, Dentistry and Pharmaceutical Sciences
[3]倉敷廣済病院整形外科．Yoshihisa Nasu: Department of Orthopaedic Surgery, Kurashiki Kosai Hospital

RA 関連手術の動向

岡山大学病院整形外科および関連病院 1 施設(倉敷廣済病院)で 2004 年 1 月から 2011 年 6 月までに行われた関節リウマチ関連手術 921 件について調査した．同一患者が同一日に複数関節(部位)の手術を受けていた場合は主たる手術手技のみを 1 件としてカウントした．対象は RA 患者 464 例(男性 41 例，女性 423 例)で手術時平均年齢は 61.7 歳，手術時平均罹病期間は 20.0 年であった．生物学的製剤非使用患者の手術は 766 件(手術時平均年齢 63.0 歳，手術時平均罹病期間 20.6 年)，生物学的製剤使用中患者の手術は 155 件(手術時平均年齢 56.2 歳，手術時平均罹病期間 17.1 年)であり，生物学的製剤使用中患者は有意に年齢が低く，罹病期間が短かった(いずれも $p<0.05$, Mann-Whitney U test)．生物学的製剤使用・非使用別の手術時平均年齢を表 1 に，平均罹病期間の年度別推移を表 2 に

表 1 2004 年～2011 年における RA 関連手術例の年度毎の手術時平均年齢

生物学的製剤使用	2004	2005	2006	2007	2008	2009	2010	2011
あり		56.7	52.4	51.2	54.1	58.8	57.1	61.4
なし	62.3	62.8	63.4	63.5	63.3	61.1	64.3	63.4
総計	62.3	62.5	61.9	61.6	61.5	60.5	61.8	62.6

(歳)

表 2 2004 年～2011 年における RA 関連手術例の年度毎の手術時平均罹病期間

生物学的製剤使用	2004	2005	2006	2007	2008	2009	2010	2011
あり		126.7	188.5	225.8	162.3	213.5	243.6	183.4
なし	230.4	241.6	268.3	248.7	244.6	247.0	262.1	240.7
総計	230.4	235.8	257.4	245.1	229.3	238.2	255.6	219.5

(月)

表 3 2004 年～2010 年の各年度における手術件数とその背景の推移

	2004	2005	2006	2007	2008	2009	2010
手術件数	127	141	133	111	125	112	121
手術時平均年齢	62.3	62.5	61.9	61.6	61.5	60.5	61.8
平均罹病期間	230.4	235.8	257.4	245.1	229.3	238.2	255.6
上肢	53 (41.7)	42 (29.8)	57 (42.9)	47 (42.3)	51 (40.8)	58 (51.8)	50 (41.3)
下肢	66 (52.0)	89 (63.1)	69 (51.9)	57 (51.3)	68 (54.4)	48 (42.8)	64 (52.3)
脊椎	8 (6.3)	10 (7.1)	7 (5.3)	7 (6.3)	6 (4.8)	6 (5.4)	7 (5.8)

示す．興味深いことに生物学的製剤使用患者での手術時年齢は近年，非使用患者と差がなくなりつつあり，生物学的製剤を適応する患者年齢が高くなりつつあることが推察される．

2011 年を除く 2004-2010 年の 1-12 月の各年度において，RA に対する整形外科手術件数は年間 110-130 件前後(平均 124.3 件)で推移しており，大きな変化はなかった(表 3)．各年度の手術総数に占める上肢，下肢，脊椎の手術が占める比率にも変化はなかった．これは Yasui らの独立行政法人国立病院機構のデータベース(NinJa)の解析結果と同様である[10]．全手術を人工関節置換術(肩，肘，膝，股関節)，手部の手術(指人工関節を含む)，足部の手術，関節鏡視下滑膜切除術，絶対的適応の手術(感染，脊椎脊髄障害，外傷)，その他に分類し，年度別動向を図 1 および表 3 に示す．人工関節手術については 2006 年から 2008 年にかけてやや減少傾向にあったが，手足の手術はかえって増加傾向にあった．この傾向は，われわれの施設を含む他施設共同研究(CORE study)による RA 関連手術の動向に類似していた[11]．さらに生物学的製剤使用・非使用に分けて手術部位・術式別の施行頻度を比較検討すると，生物学的製剤使用患者においては非使用患者に比して，人工関節置換術は少なく，手足の手術，関節鏡視下滑膜切除術は多く，絶対的適応の手術に差がない傾向がみられた(表 4)．

生物学的製剤使用下での手術

2004 年 1 月から 2011 年 6 月までの生物学的製剤投与下での整形外科手術 89 例 155 件について，使用中の生物学的製剤ごとの年度別手術件数を表 5 に，手術

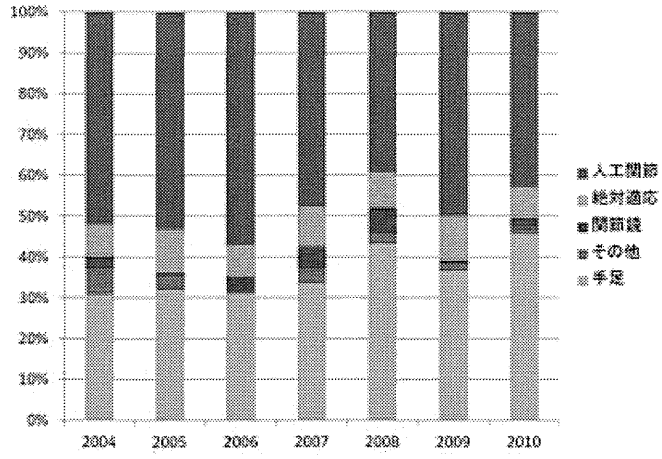

図 1　RA 関連手術の年度別動向．全 RA 関連手術を人工関節置換術(肩，肘，膝，股関節)，手部の手術(指人工関節を含む)，足部の手術，関節鏡視下滑膜切除術，絶対的適応の手術(感染，脊椎脊髄障害，外傷)，その他に分類し，2004 年 1 月から 2010 年 12 月までの各年度におけるそれぞれの比率を示した．

表 4　生物学的製剤使用の有無での手術内容

手術分類	生物学的製剤あり	生物学的製剤なし	合計
人工関節置換術	51 (32.9%)	319 (41.6%)	370
TEA	8	98	106
THA	15	63	78
TKA	26	153	179
TSA	2	5	7
手部	44 (28.4%)	188 (24.5%)	232
指人工関節	15	64	79
手関節(腱断裂を含む)	9	76	85
手指形成術	20	48	68
足部	36 (23.2%)	142 (18.5%)	178
前足部形成術	31	120	151
足関節・中後足部	5	22	27
鏡視下滑膜切除術	11 (7.1%)	19 (2.5%)	30
脊椎	4 (2.6%)	50 (6.5%)	54
外傷	2 (1.3%)	3 (0.4%)	5
感染	4 (2.6%)	21 (2.7%)	25
その他	3	29	33
合計	155	766	921

数，手術時平均年齢，平均罹病期間を表 6 に示す．使用していた生物学的製剤はインフリキシマブ 28 例 42 件，エタネルセプト 38 例 79 件，アダリムマブ 9 例 14 件，トシリズマブ 11 例 17 件，アバタセプト 3 例 3 件であり，本邦での導入が早いインフリキシマブ，エタネルセプト使用中手術の手術件数が多い結果となっている．一方で 2008 年に導入されたアダリムマブおよびトシリズマブ，2010 年に導入されたアバタセプトの手術時平均年齢は前 2 者に比して高くなっており，比較的高齢者にも生物学的製剤が導入されるように変

表 5 使用中の生物学的製剤別の手術件数の推移

	本邦での認可(年)	2004	2005	2006	2007	2008	2009	2010	2011*	計
インフリキシマブ	2003	0		3	4	8	14	10	3	42
エタネルセプト	2005	0	4	15	13	15	10	18	4	79
アダリムマブ	2008	0	2**	0	0	1	1	6	4	14
トシリズマブ	2008	0	1**	0	0	0	4	7	5	17
アバタセプト	2010	0	0	0	0	0	0	0	3	3
総計		0	7	18	17	24	29	41	19	155
総手術数に対する割合(%)		0	5.0	13.5	15.3	19.2	25.9	33.9	35.8	16.8

*2011 年 1 月- 6 月の 6 カ月間のデータ
**治験中の手術

表 6 使用中の生物学的製剤別の総手術件数と患者背景

	手術数	症例数	年齢平均	SD	平均罹病期間(月)	SD
インフリキシマブ	42	28	55.7	12.0	190.8	94.8
エタネルセプト	79	38	54.2	13.0	220.1	131.8
アダリムマブ	14	9	62.6	11.0	149.4	115.7
トシリズマブ	17	11	59.3	13.8	215.2	146.3
アバタセプト	3	3	67.0	19.1	216.0	0.0
総計	155	89	56.2	13.1	204.9	124.4

化してきた可能性がある．また，NinJa の解析結果からも，年間の RA 関連手術のうち生物学的製剤投与中の患者の割合は毎年漸増しており，2007 年は 9.7%であったことが報告されている[10]．われわれの検討結果も同様であり，2009 年度は 25.9%と約 4 人に 1 人，2010 年度は 33.9%と約 3 人に 1 人が生物学的製剤使用中であった．本邦における生物学的製剤の普及率が上昇してきたこともあるが，最近はこれを明らかに上回っており，治療に積極的な RA 患者における生物学的製剤の使用率が高くなってきていると解釈することもできる．

手術分類別の患者背景

われわれはいずれの手術においても，従来からの整形外科的治療介入の適応を変更していない．しかし，生物学的製剤使用中の患者では，以前のように関節破壊が非常に高度となってから手術を希望するのではなく，むしろ関節の不可逆的変化が，日常生活動作や美容的な障害となった時点での手術が増加しており，より軽症化している．これは，生物学的製剤を使用する患者が tight control 下にあること，高い有効性によって全身の多関節症状が緩和して愁訴がしぼられ，より高い ADL(activities of daily living)を要求するようになったことなどが考えられる．手術分類別に各患者群における RA 罹病期間と術前 CRP 値との分布を調査し，それぞれの患者背景から推察できる生物学的製剤使用下での手術の意義と適応について考察した(図 2)．

1) 滑膜切除術

Kanbe らはインフリキシマブ使用中に行った鏡視下滑膜切除術の効果を術後 6 週および 50 週で検討し，血清 CRP，DAS28 による総合的疾患活動性指標の改善をみたことを報告している．滑膜切除術は炎症性サイトカインを産生する滑膜組織を減少させることによって，当該関節における生物学的製剤の効果を改善させる可能性がある．しかし，滑膜切除術の良好な短期成績は以前から認識されており，長期的には関節破

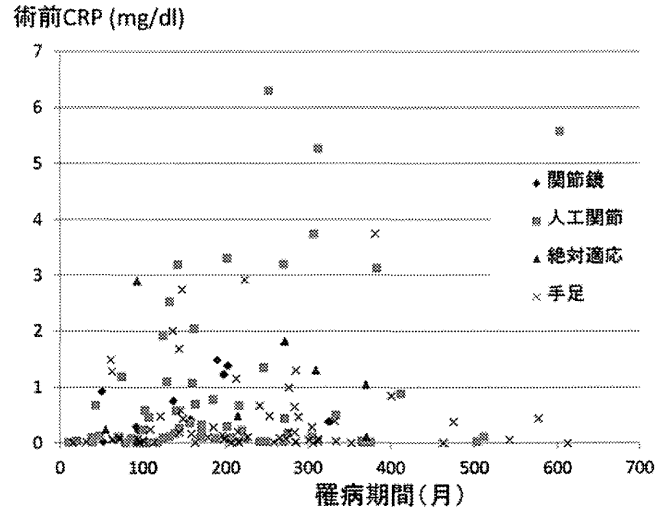

図2　生物学的製剤使用中手術の背景．2004年1月から2011年6月に行った生物学的製剤使用中手術155件を，人工関節置換術(肩，肘，膝，股関節)，手足の手術(指人工関節を含む)，関節鏡視下滑膜切除術，絶対的適応の手術(感染，脊椎脊髄障害，外傷)に分け，罹病期間，手術前CRP値(mg/dl)による分布を示した．

壊防止効果には期待できないとする意見が多い．今後問題となるのは生物学的製剤による治療に鏡視下滑膜切除術を併用することで長期的な治療効果が維持できるか否か，その限界はどこか，である．

今回調査した症例は関節形成術に併用した滑膜切除術を除く11例であり，全例が鏡視下滑膜切除術(膝9件，肘2件)であった．内訳は男性1例，女性10例，手術時平均年齢は53.2歳，平均罹病期間は6.7年と比較的若年で罹病期間が短かった．術前平均CRPは1.83 mg/dlであり，全例で薬物療法でも改善しない限局した滑膜炎が持続する場合に適応されていた．術後経過観察期間は平均32.8カ月であり，人工関節置換術をエンドポイントとしてKaplan-Meyer法による5年生存率は51.7%であった．人工関節置換術に移行した4例(3膝，1肘)はいずれも術前Larsen gradeはIIIおよびIVであり，軟骨破壊が進行すると，滑膜切除術の有効性は炎症の一時的な沈静化にとどまり，生物学的製剤使用によっても関節破壊の進行を防止することはできない場合が多い．一方，Larsen grade Iに対する滑膜切除術4例(2膝，2肘)は術後成績が維持されており，滑膜切除術は大関節では関節軟骨が障害される前の早期によりよい適応があると考えられる．

2) 人工関節置換術

人工関節置換術群51件の内訳は肩2件，肘8件，膝26件，股15件であり，平均罹病期間は215.3カ月であった．罹病期間10年未満の症例は10例14件であり，ほぼ全例で生物学的製剤導入前にすでに進行した関節破壊のある患者で，種々の程度の不可逆的な身体機能障害を有していた．平均CRP値は1.06 mg/dlであり，全身コントロールが得られている症例，生物学的製剤によっても低～中等度疾患活動性が残存した症例がほとんどであり，術前CRP高値例は生物学的製剤の二次無効例，休薬期間中の再燃であった．すでに関節破壊を有する例では，低疾患活動性にもかかわらず関節破壊の進行がゼロにできない例も認められ，生物学的製剤導入後にLarsen gradeがIIIからIVに進行して人工関節置換術に至った例やLarsen grade IVの同じGrade内で関節破壊が進行し，疼痛や不安定性が増強したために手術に至った例が含まれていた．一方，構造的破壊が軽度である早期～進行期RAの中には，経年的に関節破壊，変形が進行してくる症例も散見され，今後増加してくる患者群であると考えられた．

これらの症例から生物学的製剤使用中患者の人工関節置換術のタイミングは，①生物学的製剤導入時にすでに破壊が進行して修復の見込みのない場合，②残存

する炎症により長期の間に関節破壊が進行する場合，③大関節においてはLarsen grade III以上となって軟骨が消失した場合(ただし，肩関節，足関節では関節のリモデリングをみることがある)，④上肢においては整容，トイレ動作など基本的ADLが障害され，下肢では歩行能力が著しく低下した場合，などであり，当然骨欠損が比較的軽度で，軟部組織の破綻(腱板，側副靱帯など)や拘縮(筋，関節包，靱帯など)を来す前の手術が成績もよい．

3) 手・足の手術

手・足の手術群は80件であり，大関節に比して疼痛によるVAS(visual analogue scale)は低く，術前CRPは平均0.72 mg/dlと他の手術群に比べてもっとも疾患活動性がコントロールされていた．しかし，手術時年齢や罹病期間は人工関節手術と同等であり，10年以上の長期罹病患者が80例中61例と4分の3を占めていた．臨床的寛解・低疾患活動性となった状態での残存HAQが認められる場合に手術を希望しており，そのタイミングとしては，①変形や可動域制限のため日常生活に困る場合，②機械的刺激による疼痛が強い場合，③腱断裂や末梢神経障害，④美容的愁訴が強い場合，④外傷，骨関節感染など，が認められた．われわれは，術後も生物学的製剤の関節破壊防止効果や修復効果を期待して，手関節においては橈骨月状骨間部分固定術やSauvé-Kapandji手術，中後足部選択的固定術，中足骨短縮骨切り術など，破壊を免れた周辺関節を温存する術式を選択するようにしており，今後もこういった症例が増加していくものと思われる．

今後の展望

生物学的製剤の登場により，RAに対する整形外科手術はより理想的な状況で行われるようになったことは疑いがない．炎症の状態がコントロールされることで，貧血は改善し，切除すべき炎症性滑膜の量は減少している場合が多い．人工関節の設置に際しては骨質もよく，長期成績の改善も期待できる．今後は術前からの合併症も減少傾向になるであろう．手術の対象となる関節以外の関節は比較的良好に保たれ，より円滑なリハビリテーションが施行できる．残存する障害された関節を再建する手術治療を薬物治療に組み合わせていくことは，生物学的製剤の有効性に限界があることからも，寛解や低疾患活動性を目指す治療(treat to target, T2T)[12]のためには必須の治療戦略と思われる．わが国においては，整形外科医が積極的にRA治療にかかわってきたという独自の背景がある．われわれ整形外科医は，海外よりもたらされたT2Tに対して，薬物治療に適宜手術療法・リハビリテーションを組み入れて行う“Japanese T2T”の構築を行っていく責務がある．

一方，こういった強力な免疫抑制療法下にある患者の手術に際しては，手術部位感染(surgical site infection, SSI)が最も重要な問題となる．日本整形外科学会リウマチ委員会では2004年1月から2008年11月の間に行ったRA関連手術について，全国研修施設を対象にアンケート調査を実施した．この中で，RA関連手術59807件中，生物学的製剤使用中の手術は3468件(5.8%)であった．これら手術を行ったのは1245施設中430施設(34.5%)であり，施設間の偏りはみられるが，今後も生物学的製剤使用下の手術は増加してくるものと考えられる．一方，SSIは46件(1.3%)で，生物学的製剤非使用群の感染合併率1.0%(56339件中567件)と有意な差を認めなかったが，人工関節置換術施行例ではオッズ比2.12で生物学的製剤使用中手術にSSIが多いことが判明しており，従来のRA関連手術の際以上の注意が必要である[12]．

文　献

1) van der Heijde D, Klareskog L, Rodriguez-Valverde V, et al. Comparison of etanercept and methotrexate, alone and combined, in the treatment of rheumatoid arthritis: two-year clinical and radiographic results from the TEMPO study, a double-blind, randomized trial. Arthritis Rheum 2006; 54: 1063-74.
2) Breedveld FC, Weisman MH, Kavanaugh AF, et al. The PREMIER study: A multicenter, randomized, double-blind clinical trial of combination therapy with adalimumab plus methotrexate versus methotrexate alone or adalimumab alone in patients with early, aggressive rheumatoid arthritis who had not had previous methotrexate treatment. Arthritis Rheum 2006; 54: 26-37.
3) Nishimoto N, Hashimoto J, Miyasaka N, et al. Study of active controlled monotherapy used for rheumatoid arthritis, an IL-6 inhibitor (SAMURAI): evidence of clinical and radiographic benefit from an X ray reader-blinded randomised controlled trial of tocilizumab. Ann Rheum Dis 2007; 66: 1162-7.
4) van der Kooij SM, le Cessie S, Goekoop-Ruiterman YP, et al. Clinical and radiological efficacy

of initial vs delayed treatment with infliximab plus methotrexate in patients with early rheumatoid arthritis. Ann Rheum Dis 2009; 68: 1153-8.
5) Emery P, Durez P, Dougados M, et al. Impact of T-cell costimulation modulation in patients with undifferentiated inflammatory arthritis or very early rheumatoid arthritis: a clinical and imaging study of abatacept (the ADJUST trial). Ann Rheum Dis 2009; 69: 510-6.
6) Fevang BT, Lie SA, Havelin LI, et al. Reduction in orthopedic surgery among patients with chronic inflammatory joint disease in Norway, 1994-2004. Arthritis Rheum 2007; 57: 529-32.
7) Pedersen AB, Johnsen SP, Overgaard S, et al. Total hip arthroplasty in Denmark: incidence of primary operations and revisions during 1996-2002 and estimated future demands. Acta Orthop 2005; 76: 182-9.
8) Sokka T, Kautiainen H, Hannonen P. Stable occurrence of knee and hip total joint replacement in Central Finland between 1986 and 2003: an indication of improved long-term outcomes of rheumatoid arthritis. Ann Rheum Dis 2007; 66: 341-4.
9) Weiss RJ, Ehlin A, Montgomery SM, et al. Decrease of RA-related orthopaedic surgery of the upper limbs between 1998 and 2004: data from 54,579 Swedish RA inpatients. Rheumatology (Oxford) 2008; 47: 491-4.
10) Yasui T, Nishino J, Kadono Y, et al. Impact of biologics on the prevalence of orthopedic surgery in the National Database of Rheumatic Diseases in Japan. Mod Rheumatol; 20: 233-7.
11) Momohara S, Tanaka S, Nakamura H, et al. Recent trends in orthopedic surgery performed in Japan for rheumatoid arthritis. Mod Rheumatol2011; 21: 337-42.
12) Suzuki M, Nishida K, Soen S, et al. Risk of postoperative complications in rheumatoid arthritis relevant to treatment with biologic agents: a report from the Committee on Arthritis of the Japanese Orthopaedic Association. J Orthop Sci 2011; 16: 778-84.

Functional Variants in *NFKBIE* and *RTKN2* Involved in Activation of the NF-κB Pathway Are Associated with Rheumatoid Arthritis in Japanese

Keiko Myouzen[1], Yuta Kochi[1,2]*, Yukinori Okada[1,2,3], Chikashi Terao[4,5], Akari Suzuki[1], Katsunori Ikari[6], Tatsuhiko Tsunoda[7], Atsushi Takahashi[3], Michiaki Kubo[8], Atsuo Taniguchi[6], Fumihiko Matsuda[4,9,10], Koichiro Ohmura[5], Shigeki Momohara[6], Tsuneyo Mimori[5], Hisashi Yamanaka[6], Naoyuki Kamatani[11], Ryo Yamada[12], Yusuke Nakamura[13], Kazuhiko Yamamoto[1,2]

1 Laboratory for Autoimmune Diseases, Center for Genomic Medicine (CGM), RIKEN, Yokohama, Japan, **2** Department of Allergy and Rheumatology, Graduate School of Medicine, the University of Tokyo, Tokyo, Japan, **3** Laboratory for Statistical Analysis, CGM, RIKEN, Yokohama, Japan, **4** Center for Genomic Medicine, Kyoto University Graduate School of Medicine, Kyoto, Japan, **5** Department of Rheumatology and Clinical Immunology, Graduate School of Medicine, Kyoto University, Kyoto, Japan, **6** Institute of Rheumatology, Tokyo Women's Medical University, Tokyo, Japan, **7** Laboratory for Medical Informatics, CGM, RIKEN, Yokohama, Japan, **8** Laboratory for Genotyping Development, CGM, RIKEN, Yokohama, Japan, **9** CREST Program, Japan Science and Technology Agency, Kawaguchi, Saitama, Japan, **10** Institut National de la Santé et de la Recherche Médicale (INSERM), Unité U852, Kyoto University Graduate School of Medicine, Kyoto, Japan, **11** Laboratory for International Alliance, CGM, RIKEN, Yokohama, Japan, **12** Unit of Statistical Genetics, Center for Genomic Medicine, Graduate School of Medicine, Kyoto University, Kyoto, Japan, **13** Laboratory of Molecular Medicine, Human Genome Center, Institute of Medical Science, University of Tokyo, Tokyo, Japan

Abstract

Rheumatoid arthritis is an autoimmune disease with a complex etiology, leading to inflammation of synovial tissue and joint destruction. Through a genome-wide association study (GWAS) and two replication studies in the Japanese population (7,907 cases and 35,362 controls), we identified two gene loci associated with rheumatoid arthritis susceptibility (*NFKBIE* at 6p21.1, rs2233434, odds ratio (OR) = 1.20, $P = 1.3 \times 10^{-15}$; *RTKN2* at 10q21.2, rs3125734, OR = 1.20, $P = 4.6 \times 10^{-9}$). In addition to two functional non-synonymous SNPs in *NFKBIE*, we identified candidate causal SNPs with regulatory potential in *NFKBIE* and *RTKN2* gene regions by integrating *in silico* analysis using public genome databases and subsequent *in vitro* analysis. Both of these genes are known to regulate the NF-κB pathway, and the risk alleles of the genes were implicated in the enhancement of NF-κB activity in our analyses. These results suggest that the NF-κB pathway plays a role in pathogenesis and would be a rational target for treatment of rheumatoid arthritis.

Citation: Myouzen K, Kochi Y, Okada Y, Terao C, Suzuki A, et al. (2012) Functional Variants in *NFKBIE* and *RTKN2* Involved in Activation of the NF-κB Pathway Are Associated with Rheumatoid Arthritis in Japanese. PLoS Genet 8(9): e1002949. doi:10.1371/journal.pgen.1002949

Editor: Panos Deloukas, The Wellcome Trust Sanger Institute, United Kingdom

Received March 31, 2012; **Accepted** July 12, 2012; **Published** September 13, 2012

Funding: This work was conducted as a part of the BioBank Japan Project that was supported by the Ministry of Education, Culture, Sports, Sciences, and Technology of the Japanese government. The funders had no role in study design, data collection and analysis, decision to publish, or preparation of the manuscript.

Competing Interests: The authors have declared that no competing interests exist.

* E-mail: ykochi@src.riken.jp

Introduction

Rheumatoid arthritis (RA [MIM 180300]) is an autoimmune disease [1] with a complex etiology involving several genetic factors as well as environmental factors. Previous genome-wide association studies (GWAS) for RA have discovered many genetic loci [2–6], although the causal mechanisms linking the variants in these loci and disease etiology are largely unknown, except for in a few cases [6–8]. In contrast to mutations in Mendelian, monogenic diseases, most disease-associated variants in complex diseases, including autoimmune diseases, have moderate effects on disease susceptibility. This is because the disease causal variants in complex diseases are thought to have moderate effects on gene function, while amino acid changes introduced by the mutations of monogenic diseases have critical impacts on protein function [9]. Moreover, it has been demonstrated that the majority of autoimmune disease loci are expression quantitative trait loci (eQTLs) [10,11], indicating that accumulation of quantitative, but not qualitative, changes in gene function likely predisposes individuals to the disease. This renders it difficult to pinpoint the causal variants in the GWAS loci, especially in eQTLs, because all the variations in strong linkage disequilibrium (LD) with the marker SNP in a GWAS, the majority of which are not covered by the SNP array, are possible candidates for causal variants.

In recent years, with the emergence of next-generation sequencing technologies, the way we approach disease-causing variants has dramatically changed. First, a comprehensive map of human genetic variations is now available owing to the 1000 Genome Project [12], which allows us to grasp most of the potential common variants. This also enables us to perform genotype imputation of SNPs that are not directly genotyped in the GWAS, and consequently, to test them for association. Second, genomic studies using new technologies, such as chromatin immunoprecipitation-sequencing (ChIP-seq) and DNase I hypersensitive sites sequencing (DNase-seq), have advanced our understanding of how each genomic cluster regulates gene

Author Summary

Rheumatoid arthritis (RA) is a chronic autoimmune disease affecting approximately 1% of the general adult population. More than 30 susceptibility loci for RA have been identified through genome-wide association studies (GWAS), but the disease-causal variants at most loci remain unknown. Here, we performed replication studies of the candidate loci of our previous GWAS using Japanese cohorts and identified variants in *NFKBIE* and *RTKN2* gene loci that were associated with RA. To search for causal variants in both gene regions, we first examined non-synonymous (ns)SNPs that alter amino-acid sequences. As *NFKBIE* and *RTKN2* are known to be involved in the NF-κB pathway, we evaluated the effects of nsSNPs on NF-κB activity. Next, we screened *in silico* variants that may regulate gene transcription using publicly available epigenetic databases and subsequently evaluated their regulatory potential using *in vitro* assays. As a result, we identified multiple candidate causal variants in *NFKBIE* (2 nsSNPs and 1 regulatory SNP) and *RTKN2* (2 regulatory SNPs), indicating that our integrated *in silico* and *in vitro* approach is useful for the identification of causal variants in the post–GWAS era.

transcription. If disease-associated variants are present in a critical site for gene regulation suggested by the ChIP-seq and DNase-seq studies, the disease-associated variants might possibly influence gene transcription levels such as through altered transcription factor-DNA binding avidity.

In the present study, we first performed replication studies of candidate loci in our previous GWAS and identified two association signals with genome-wide significance ($P<5\times10^{-8}$) in nuclear factor of kappa light polypeptide gene enhancer in B-cells inhibitor, epsilon (*NFKBIE* [MIM 604548]) and rhotekin 2 (*RTKN2*) loci. By utilizing publicly available datasets yielded by the above-mentioned genomic studies, we then performed integrated *in silico* and *in vitro* analysis to identify plausible causal variants in *NFKBIE* and *RTKN2* loci.

Results

Identification of rheumatoid arthritis susceptibility genes

We previously performed a GWAS of RA using a Japanese case-control cohort (2,303 cases and 3,380 controls) and identified significant associations in major histocompatibility complex, class II, DR beta 1 (*HLA-DRB1* [MIM 142857]), and chemokine (C-C motif) receptor 6 (*CCR6* [MIM 601835]) loci ($P_{GWAS}<5\times10^{-8}$) [6]. To reveal additional risk loci from those showing moderate associations in the GWAS (31 loci, $5\times10^{-8}<P_{GWAS}<5\times10^{-5}$), we selected a landmark SNP from each locus and genotyped it for an additional cohort (replication-1: 2,187 cases and 28,219 controls) (Table S1, S2). Among the 31 SNPs genotyped, seven SNPs were nominally associated with RA ($P<0.05$), which included SNPs in the tumor necrosis factor, alpha-induced protein 3 (*TNFAIP3* [MIM 191163]), and signal transducer and the activator of transcription 4 (*STAT4* [MIM 600558]) gene loci that were previously reported to be associated with RA [13,14] (Table S2). In a combined analysis of the GWAS and the 1st replication study, we identified two associations with genome-wide significance ($P<5\times10^{-8}$) in *NFKBIE* (6p21.1, rs2233434, $P=4.1\times10^{-11}$, odds ratio (OR) = 1.21, 95% confidence interval (CI) = 1.14–1.28) and in *RTKN2* (10q21.2, rs3125734, $P=3.7\times10^{-8}$, OR = 1.23, 95% CI = 1.14–1.32) (Table 1 and Figure 1). *NFKBIE* was previously reported as a novel RA susceptibility gene locus in a meta-analysis of three GWASs for RA in the Japanese population, which included the GWAS set that the present study used [15]. *RTKN2* is located in the same region (10q21) as *ARID5B*, in which a significant association signal was also reported in the meta-analysis [15]. In our GWAS set, however, two significant signals were observed at rs3125734 (*RTKN2*: $P=4.8\times10^{-5}$) and rs10821944 (*ARID5B*: $P=7.4\times10^{-4}$), the former of which was tested as a landmark in the replication study. These two SNPs were in weak LD ($r^2=0.11$) and the independent effect of each SNP was observed after conditioning on each SNP (*RTKN2*: $P=1.5\times10^{-3}$, *ARID5B*: $P=0.024$, respectively). This indicated that two independent associations existed in this region, and the association of *RTKN2* is novel. We also confirmed the association in the *STAT4* locus [14] with genome-wide significance (2q32.2, rs10168266, $P=3.2\times10^{-8}$, OR = 1.16, 95% CI = 1.10–1.22) (Table S2). The associations in *NFKBIE* and *RTKN2* were further replicated in the 2nd replication cohort (3,417 cases and 3,763 controls; rs2233434, $P=1.1\times10^{-5}$, OR = 1.19, 95% CI = 1.10–1.30 and rs3125734, $P=0.016$, OR = 1.14, 95% CI = 1.02–1.26, respectively), confirming the associations in these loci (a combined analysis of three sets; rs2233434, $P=1.3\times10^{-15}$, OR = 1.20, 95% CI = 1.15–1.26 and rs3125734, $P=4.6\times10^{-9}$, OR = 1.20, 95% CI = 1.13–1.27, respectively) (Table 1 and Figure 1). We also genotyped these SNPs for individuals with systemic lupus erythematosus (SLE [MIM 152700]) ($n=657$) and Graves' disease (GD [MIM 275000]) ($n=1,783$). We identified a significant association of *RTKN2* (rs3125734) with GD ($P=3.4\times10^{-5}$, OR = 1.24, 95% CI = 1.12–1.37), whereas no significant associations were detected in *NFKBIE* (rs2233434) with either disease or in *RTKN2* (rs3125734) with SLE (Table S3).

Functional analysis of non-synonymous SNPs

NFKBIE and *RTKN2* genes are both involved in the NF-κB pathway: *NFKBIE* encodes IκB epsilon (IκBε), a member of the IκB family [16], and its binding to NF-κB inhibits the nuclear translocation of NF-κB [17]; *RTKN2* encodes a member of Rho-GTPase effector proteins highly expressed in $CD4^+$ T cells [18] and is implicated in the activation of the NF-κB pathway [19]. Considering that the NF-κB pathway is critical for the pathogenesis of RA [20], these two genes could be strong candidates in these regions. To identify disease-causing variants, we first sequenced the coding regions of the genes using DNA from patients ($n=48$) to find variants that alter amino acid sequences. We identified four non-synonymous (ns)SNPs, which were all registered in the dbSNP database: two nsSNPs in *NFKBIE* (rs2233434 (Val194Ala) and rs2233433 (Pro175Leu)) and two in *RTKN2* (rs3125734 (Arg462His) and rs61850830 (Ala288Thr)), where rs2233434 and rs3125734 were the same as the landmark SNPs in the GWAS (Figure 1 and Figure 2A). The two nsSNPs of each locus were in strong LD (Figure 2B) and were both associated with disease (Table S4). In the haplotype analysis, a single common risk haplotype with a frequency >0.05 was observed in each locus, and significant associations with disease risk were detected (*NFKBIE*, $P=5.3\times10^{-8}$, Table S5; *RTKN2*, $P=5.7\times10^{-5}$, Table S6).

To investigate the effect of these nsSNPs on protein function, we evaluated them by *in silico* analysis using PolyPhen and SIFT software, which predicts possible impacts of amino acid substitutions on the structure and function of proteins, but all four nsSNPs were predicted to have little effect (Table S7), contrasting with the effect of Mendelian disease mutations [9]. We next examined their influence on the NF-κB activity in cells by performing NF-κB

Table 1. Association analysis of *NFKBIE* and *RTKN2* with rheumatoid arthritis.

Gene	dbSNP ID	Allele (1/2)	Study set	Number of subjects		Frequency of allele 1		Odds ratio (95% CI)	*P*-value[a]
				Case	Control	Case	Control		
NFKBIE	rs2233434	G/A	GWAS	2,303	3,380	0.254	0.216	1.24 (1.13–1.35)	2.2×10^{-6}
			Replication study-1	2,186	28,204	0.245	0.215	1.19 (1.10–1.27)	4.2×10^{-6}
			Replication study-2	3,396	3,756	0.239	0.209	1.19 (1.10–1.30)	1.1×10^{-5}
			Combined analysis	7,885	35,340	0.245	0.215	1.20 (1.15–1.26)	1.3×10^{-15}
RTKN2	rs3125734	T/C	GWAS	2,303	3,380	0.125	0.101	1.27 (1.13–1.43)	4.8×10^{-5}
			Replication study-1	2,185	28,218	0.129	0.110	1.20 (1.09–1.31)	1.4×10^{-4}
			Replication study-2	3,402	3,751	0.115	0.103	1.14 (1.02–1.26)	0.016
			Combined analysis	7,890	35,349	0.122	0.108	1.20 (1.13–1.27)	4.6×10^{-9}

[a]: Cochran-Armitage trend test was used for the GWAS and replication studies. Mantel-Haenszel method was used for the combined analysis.

doi:10.1371/journal.pgen.1002949.t001

reporter assays with haplotype-specific expression vectors. In *NFKBIE*, the non-risk haplotype (A-C: rs2233434 (non-risk allele (NR))-rs2233433 (NR)) displayed an inhibitory effect on NF-κB activity compared with the mock construct, which reflected compulsorily binding of exogenous IκBε to the endogenous NF-κB, as shown in a previous study [16]. Of note, the risk haplotype (G-T: risk allele (R)-R) showed higher NF-κB activity than A-C (NR-NR) (Figure 3A), suggesting impaired inhibitory potential of G-T (R-R) products. No haplotypic difference was detected in the protein expression levels of these constructs (Figure 3C). We also examined two additional constructs of G-C (R-NR) and A-T (NR-R) haplotypes to evaluate the effect of each nsSNP (Figure S1A, S1B). Because NF-κB activity increased in the order of A-C<G-C<A-T<G-T (rs2233434-rs2233433: NR-NR<R-NR<NR-R<R-R) when cells were stimulated with TNF-α, the C>T substitution (Pro175Leu) in rs2233433 may have more impact on the protein function of IκBε compared with the A>G substitution (Val194Ala) in rs2233434. In contrast to the observations in *NFKBIE*, no clear difference was detected between the two common haplotype products of *RTKN2* in either their effect on NF-κB activity or protein expression levels, although both products enhanced NF-κB activity as reported previously (Figure 3B, 3D) [19]. These functional analyses of nsSNPs suggest that two nsSNPs (rs2233434 and rs2233433) in the *NFKBIE* region are candidates for causal SNPs.

ASTQ analysis suggested the existence of regulatory variants

As the majority of autoimmune disease loci have been implicated as eQTL [11], we speculated that variants in the *NFKBIE* and *RTKN2* loci would influence gene function by regulating gene expression, in addition to changing the amino acid sequences. To address this possibility, we performed allele-specific transcript quantification (ASTQ) analysis by using allele-specific probes targeting the nsSNPs in exons (rs2233434 for *NFKBIE* and rs3125734 for *RTKN2*, both of which were the GWAS landmarks). The genomic DNAs and cDNAs were extracted from peripheral blood mononuclear cells (PBMCs) in individuals with heterozygous genotype ($n=14$ for *NFKBIE* and $n=6$ for *RTKN2*) and from lymphoblastoid B-cell lines ($n=9$) for *NFKBIE*. As the expression levels of *RTKN2* were low in lymphoblastoid B cells, only PBMCs were used. When quantified by allele-specific probes, transcripts from the risk allele of *NFKBIE* showed 1.1-fold and 1.2-fold lower amounts (in PBMCs and lymphoblastoid B cells, respectively) than those from non-risk alleles ($P=0.012$ and 5.3×10^{-4}, respectively; Figure 3E and Figure S2). In contrast, 1.5-fold higher amounts of transcripts were observed in the risk allele of *RTKN2* ($P=0.016$; Figure 3F). These allelic imbalances suggested that both gene loci were eQTL and that there existed variants with *cis*-regulatory effects. Moreover, considering the inhibitory effects of *NFKBIE* and the activating potential of *RTKN2* on NF-κB activity, which might both be dose dependent (Figure 3G, 3H), these regulatory variants in the risk alleles should enhance NF-κB activity *in vivo*.

Integrated *in silico* and *in vitro* analysis to search for regulatory variants

To comprehensively search the two genomic regions for causal regulatory variants, we performed an integrated *in silico* and *in vitro* analysis with multiple steps (Figure 4 and Figures S3, S4). We first determined the target genomic region by selecting LD blocks containing disease-associated SNPs ($P_{GWAS}<1.0\times10^{-3}$) (Step 1). We then extracted SNPs with frequencies of >0.05 from HapMap and 1000 Genome Project databases in the region (Step 2). We excluded uncommon variants (MAF<0.05) from the analysis because of their low imputation accuracy in the GWAS (93% of uncommon variants in *NFKBIE* and 76% in *RTKN2* exhibited *Rsq* <0.6). There is neither structural variation (>1 kbps) nor indels (100 bps to 1 kbs) that are common in the population (frequency >0.01) in these loci. To evaluate the *cis*-regulatory potential of sequences around the SNPs *in silico*, we used the regulatory potential (RP) score [21,22]. This score was calculated based on the extent of sequence conservation among species or similarity with known regulatory motifs. We selected SNPs from the genomic elements with an RP score >0.1 (Step 3a). Subsequently, we selected SNPs from sites of transcriptional regulation as demonstrated by previous ChIP-seq studies (transcription factor binding sites [23,24] and histone modification sites [25,26]) or a DNase-seq study (DNase I hypersensitivity sites) [27] (Step 3b). Finally, these SNPs with regulatory potential were further screened out by the disease-association status ($P<0.05$) using an imputed GWAS dataset (Step 4). As a consequence, we selected 14 SNPs in *NFKBIE* and 10 SNPs in *RTKN2* that had regulatory potential predicted *in silico*.

To further investigate the regulatory potential of the SNPs, we evaluated 31-bp sequences around the SNPs by *in vitro* assays. First, we examined their ability to bind nuclear proteins by EMSAs (Step 5a) using nuclear extracts from lymphoblastoid B cells (PSC cells) and Jurkat cells. Of the 24 SNPs examined, nine

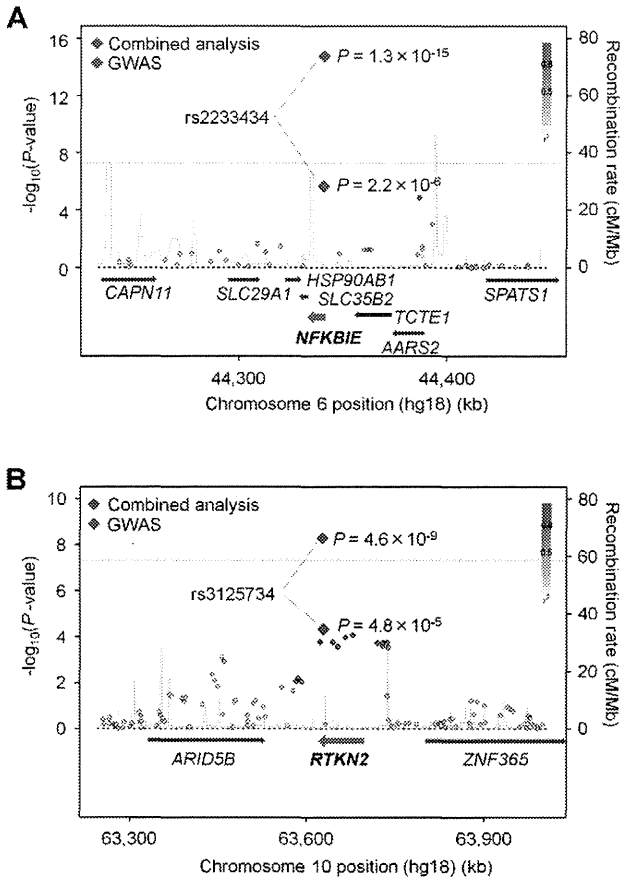

Figure 1. Association plots of *NFKBIE* and *RTKN2* regions. The diamonds represent the -$\log_{10}$ of the Cochran-Armitage trend *P*-values. Large diamonds show landmark SNPs in *NFKBIE* (rs2233434: A) and *RTKN2* (rs3125734: B). Red: GWAS, Blue: combined analysis. Red colors of each SNP indicate its r^2 with landmark SNP. Gray lines indicate the genome-wide significance threshold ($P<5\times10^{-8}$). For each plot, the -$\log_{10}$ *P*-values (y-axis) of the SNPs are presented according to their chromosomal positions (x-axis). Physical positions are based on NCBI build 36.3 of the human genome. Genetic recombination rates, estimated using the 1000 Genome Project (JPT and CHB), are represented by the blue line.
doi:10.1371/journal.pgen.1002949.g001

SNPs displayed allelic differences, implying differential potential of transcriptional activity between these alleles (Figure 5A and Figure S5). We then evaluated the enhancing or repressing activity of the sequences by luciferase reporter assays (Step 5b). We cloned them into the pGL4.24 vector, which has minimal promoter activity, and transfected these constructs into HEK293A cells (for *NFKBIE* and *RTKN2*), lymphoblastoid B cells (for *NFKBIE*), and Jurkat cells (for *RTKN2*). Among the three SNPs examined in *NFKBIE*, the risk allele of rs2233424 (located −396 bps from the 5′ end) displayed stronger repression activity (Figure 2A and Figure 5B) than that of the non-risk allele. Among the six SNPs in *RTKN2*, the risk alleles of rs12248974 (approximately 10 kb from the 3′ end) and rs61852964 (−215 bps from the 5′ end) showed higher enhancing activity compared with the non-risk alleles (Figure 2A and Figure 5B). These results corresponded to the results of ASTQ analyses (Figure 3E, 3F). Other SNPs showed no allelic differences or had the opposite trend of transcriptional activity in the risk allele compared to the results of ASTQ analysis (Figure S6).

To confirm the regulatory potential of these SNPs, we investigated the correlation between genotypes and gene expression levels in lymphocytes utilizing the data from the previous eQTL studies. We evaluated the expression of *RTKN2* in primary T cells from Western European individuals by using Genevar software [28,29]. Though *NFKBIE* is also expressed in primary T cells, the genotypes of rs2233424 are not available. We thus evaluated gene expression data of lymphoblastoid B-cell lines obtained from HapMap individuals (Japanese (JPT) + Han Chinese in Beijing (CHB), European (CEU), and African (YRI)) [30,31] instead. The *NFKBIE* expression level decreased with the number of risk alleles of rs2233424 ($R=-0.18$, $P=0.020$), and the *RTKN2* expression levels increased with that of rs1432411 (a proxy for rs12248974, $r^2=0.97$) ($R=0.27$, $P=0.018$) (Figure 5C), corresponding to the results of the *in vitro* assays. The data for rs61852964 in *RTKN2* was not available. Among the SNPs that displayed opposite transcriptional activities in the reporter assays compared to the results of ASTQ, the data for rs2233434, rs77986492, and rs3852694 (a proxy for rs1864836, $r^2=1.0$) were available (Figure S7 and S8). These SNPs displayed the opposite direction of the correlation trend as compared to the results of reporter assays, but parallel to ASTQ, implying that the regulatory effects observed in the *in vitro* assays were cancelled out by the effects of other regulatory variants on the same haplotype *in vivo*.

Finally, we validated the associations of these regulatory (r)SNPs observed in the imputed GWAS dataset. We directly genotyped them by TaqMan assay and confirmed significant associations (Table S8). As the candidate causal variants (nsSNPs and rSNPs) and the landmark SNPs of GWAS were in strong LD at each locus (Figure 2A, 2B), we evaluated the independent effect of each SNP by haplotype analysis in both loci (Table S9 and S10) and the conditional logistic regression analysis in *RTKN2* (Table S11). The conditional analysis was not performed in *NFKBIE* because three candidate causal variants were in strong LD ($r^2>0.9$). However, the analyses for these two loci did not demonstrate any evidence of primary or independent effects across the candidate causal variants, and it remains a possibility that all of the functional variants were involved in the pathogenesis. In addition, although the landmark nsSNP (rs3125734) in *RTKN2* did not display any influence on NF-κB activity in our *in vitro* assays, rs3125734 might influence functions of *RTKN2* other than those in the NF-κB pathway; alternatively, it is still possible that rs3125734 tags the effects of other unknown variants, such as rare variants, in addition to the other two rSNPs (rs12248974 and rs61852964).

Discussion

In the present study, we performed a replication study of our previously reported GWAS and identified variants in *NFKBIE* and *RTKN2* loci that were associated with RA susceptibility. The associations of *NFKBIE* and *RTKN2* loci have not been reported in other populations with genome-wide significance. However, rs2233434 in *NFKBIE* showed a suggestive association (589 cases vs. 1,472 controls, $P=0.0099$, OR = 1.57, 95% CI = 1.11–2.21) in a previous meta-analysis in European populations [32]. The weak association signal in Europeans may be partially due to the lower frequency of the risk allele (0.04 in Europeans compared to 0.22 in Japanese). On the other hand, the association of rs3125734 in *RTKN2* was not observed in a GWAS meta-analysis of European populations (cases 5,539 vs. controls 20,169, $P=0.11$, OR = 1.04, 95% CI = 0.99–1.09). As the association of *RTKN2* locus was also implicated in Graves' disease in a Han Chinese population [33], the association in *RTKN2* locus may be unique to Asian populations.

To find the disease causal variants in disease-associated loci, target re-sequencing and variant genotyping with a large sample set followed by conditional association analysis examining the

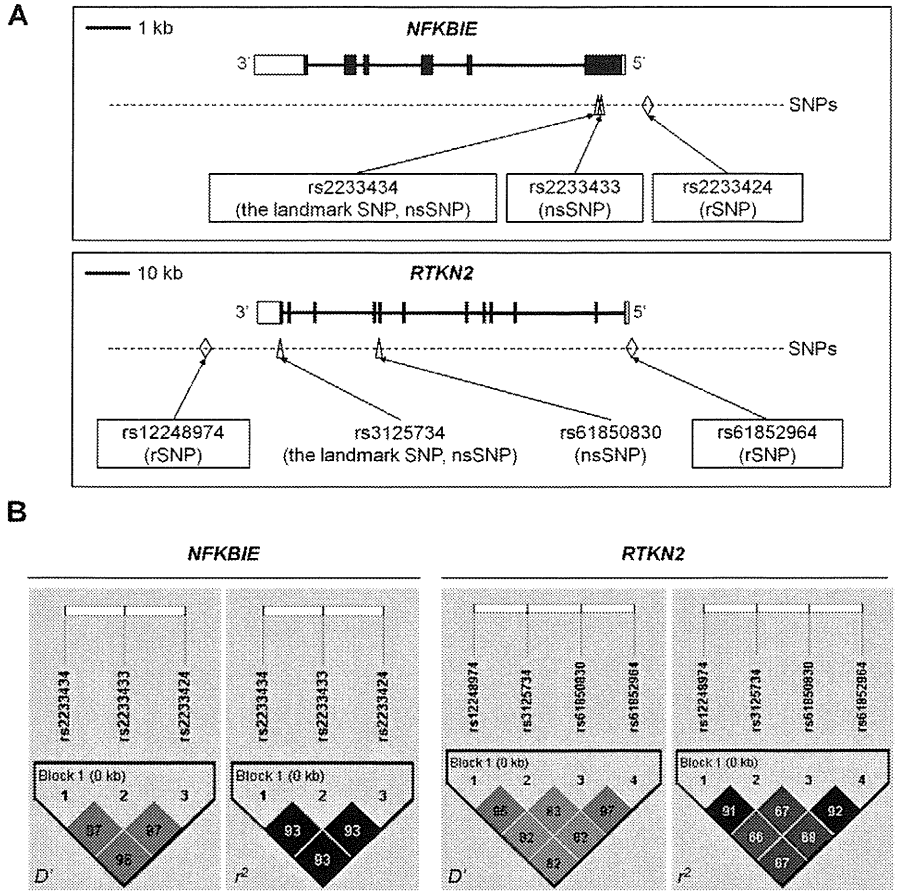

Figure 2. Genomic position and LD blocks. (A) Genomic position of non-synonymous (ns)SNPs and regulatory (r)SNPs in *NFKBIE* and *RTKN2*. *NFKBIE* (top) and *RTKN2* (bottom) correspond to transcripts NM_004556.2 and NM_145307.2, respectively. Exons are shown as boxes, where black boxes represent coding regions and open boxes represent untranslated regions. Intron sequences are drawn as lines. Open triangles represents nsSNPs and open diamond shapes indicate candidate rSNPs. dbSNP IDs of candidate causal variants were boxed in a solid line. (B) LD patterns for nsSNPs and candidate rSNPs in *NFKBIE* (left) and *RTKN2* (right) gene regions. LD blocks were constructed from genotype data of 3,290 control individuals of the GWAS. The diagrams show pairwise LD values as quantified using the D' and r^2 values.
doi:10.1371/journal.pgen.1002949.g002

independent effects of each variant would be the first step. For this purpose, a recent attempt to fine-map the known autoimmunity risk loci in Celiac disease (MIM 212750) using an "Immunochip" brought us several insights [34]. First, no stronger signals compared to the GWAS signals were detected in most of the known loci, while additional independent signals were found in several loci. Second, none of the genome-wide significant common SNP signals could be explained by any rare highly penetrant variants. Third, although the fine-mapping strategy could localize the association signals into finer scale regions, it could not identify the actual causal variants due to strong LD among the variants, indicating that an additional approach, such as functional evaluation of candidate variants, is needed.

In the present study, we focused on common variants to find causal variants. Instead of re-sequencing additional samples, we utilized the 1000 Genome Project dataset, where the theoretically estimated cover rate for common variants (frequency of >0.05) in our population is >0.99 [12,35]. To fine-map the association signals, we performed imputation-based association analysis, where we could not find any association signals that statistically exceeded the effect of landmark SNPs (rs2233434 for *NFKBIE* and rs3125734 for *RTKN2*) in both gene regions (Figures S3 and S4). We also performed a conditional logistic regression analysis, and found no additional independent signals of association when conditioned on each landmark SNP (data not shown). Although the imputation-based association tests may yield some bias compared to direct genotyping of the variants, these results suggested that variants in strong LD with the landmark SNPs were strong candidates for causal variants.

Following the analysis of nsSNPs, we evaluated *cis*-regulatory effects of variants in the two regions by ASTQ analysis using both B-cell lines and primary cells (PBMC), the majority of which consisted of T and B lymphocytes. As the mechanism of gene-regulation is substantially different between cell types [26], ASTQ analysis in more specific cell types that are relevant to the disease etiology, such as Th1 and Th17 cells, would be ideal to evaluate the *cis*-regulatory effects of variants. In this context, a more comprehensive catalog of the eQTL database of multiple cell types should be established for genetic study of diseases. As our ASTQ analysis demonstrated *cis*-regulatory effects of variants in both regions, we then performed an integrated *in silico* and *in vitro* analysis to identify candidate regulatory variants. Accumulating evidence by recent ChIP-seq and DNase-seq studies suggested that *cis*-regulatory variants are

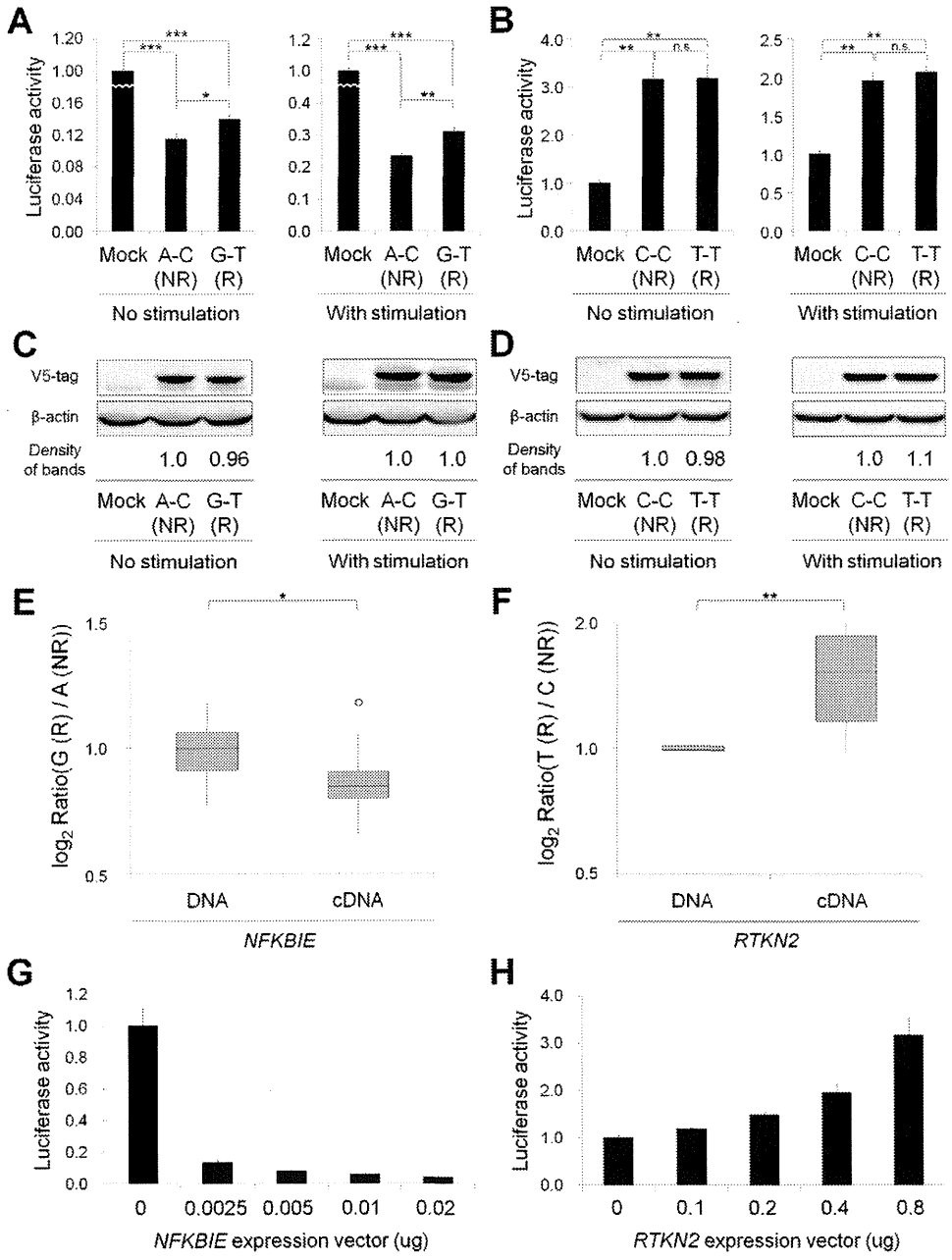

Figure 3. Functional evaluation of nsSNPs and allelic imbalance of expression in *NFKBIE* and *RTKN2*. (A, B) Effects of nsSNPs in *NFKBIE* (A) and *RTKN2* (B) on NF-κB activity by luciferase assays. Two haplotype constructs (A-C (rs2233434-rs2233433; non-risk (NR)) and G-T (risk (R)) for *NFKBIE* and C-C (rs3125734-rs61850830; NR) and T-T (R) for *RTKN2*) were used. The expression vector of each construct, pGL4.32[*luc2P*/NF-κB-RE] vector and pRL-TK vector were transfected into HEK293A cells. Data represent the mean ± s.d. Each experiment was performed in sextuplicate, and experiments were independently repeated three times. $*P<0.05$, $**P<1.0\times10^{-5}$, and $***P<1.0\times10^{-10}$ by Student's *t*-test. n.s.: not significant. (C, D) Protein expression levels of each haplotype construct. Anti-V5 tag antibody was used in the Western blotting analysis to detect the expression of exogenous IκBε (C) and RTKN2 (D). Beta-actin expression was used as an internal control. The densities of the bands were quantified and normalized to that of the risk allele. (E, F) Allelic imbalance of expression in *NFKBIE* (E) and *RTKN2* (F). ASTQ was performed using samples from individuals heterozygous for rs2233434 (G/A) in *NFKBIE* and rs3125734 (T/C) in *RTKN2*. Genomic DNAs and cDNAs were extracted from PBMCs ($n=14$ for *NFKBIE* and $n=6$ for *RTKN2*). The y-axis shows the $\log_2$ ratio of the transcript amounts in target SNPs (risk allele/non-risk allele). The top bar of the box-plot represents the maximum value and the lower bar represents the minimum value. The top of box is the third quartile, the bottom of box is the first quartile, and the middle bar is the median value. The circle is an outlier. $*P=0.012$, $**P=0.016$, by Student's *t*-test. (G, H) Dose-dependent inhibition of *NFKBIE* (G) and activation of *RTKN2* (H) on NF-κB activity. Various doses of expression vectors carrying the non-risk allele of each gene were transfected into HEK293A cells with pGL4.32 and pRL-TK vectors.
doi:10.1371/journal.pgen.1002949.g003

located in the key regions of transcriptional regulation [26,36], warranting the prioritization of variants before evaluation by *in vitro* assays. This could also minimize false-positive results of the *in vitro* assays. However, there may be additional causal variants, including rare variants, unsuccessfully selected at each step of our integrated screening. Therefore, the screening strategy

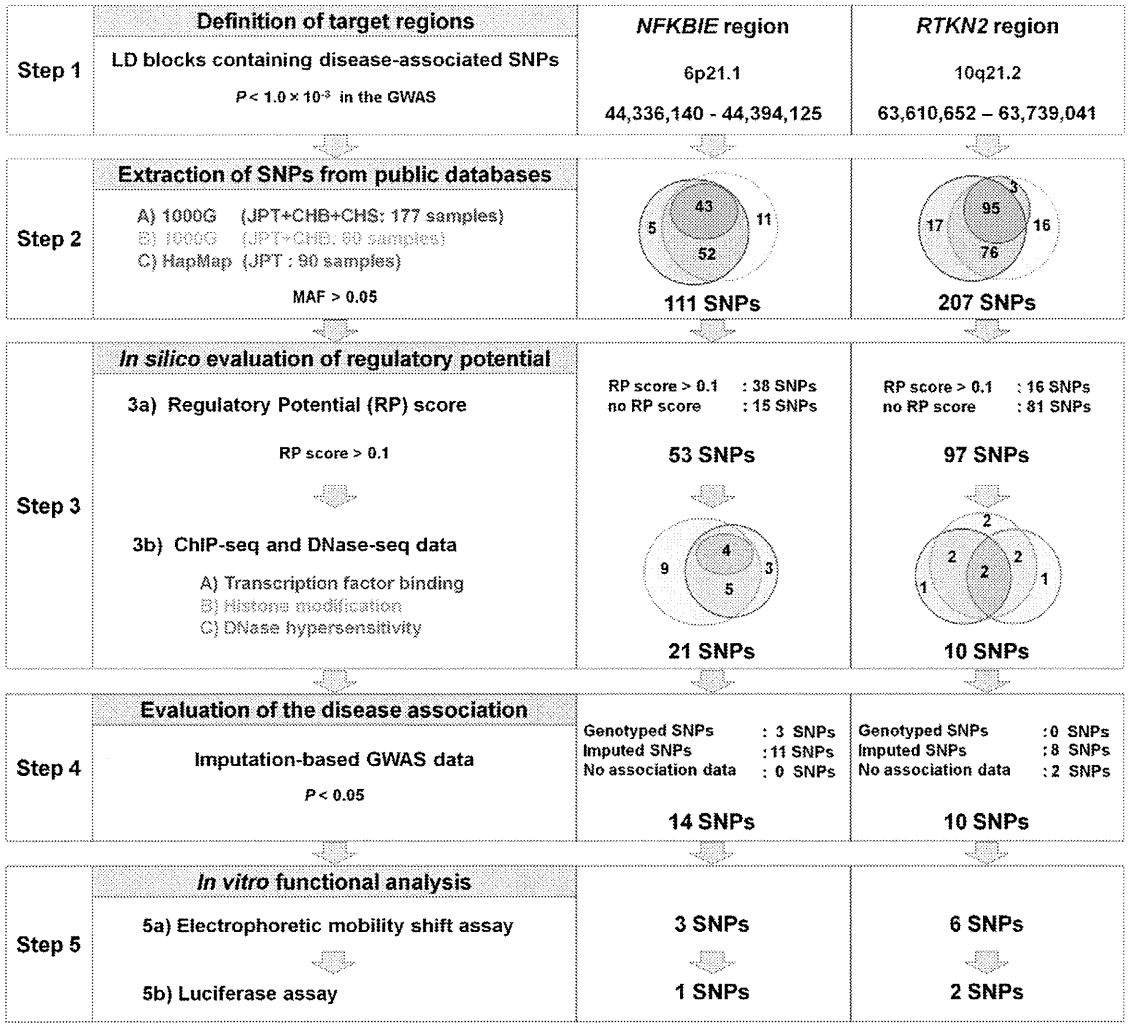

Figure 4. Overview of SNP selection using integrated *in silico* and *in vitro* approaches. The figure shows the SNP selection process (left) and the results of *NFKBIE* (middle) and *RTKN2* (right). (Step 1) LD blocks that contain disease-associated SNPs ($P_{GWAS}<1.0\times10^{-3}$) were selected. (Step 2) SNPs were extracted from three databases (A–C). 1000G, 1000 Genome Project; HapMap, International HapMap Project. A) JPT, CHB, and CHS samples ($n=177$) from the 1000G (the August 2010 release). B) JPT and CHB samples ($n=60$) from the pilot 1 low coverage study data of 1000G (the March 2010 release). C) JPT samples ($n=90$) from HapMap phase II+III (release #27). SNPs with minor allele frequency >0.05 were selected. (Step 3) Prediction of regulatory potential *in silico*. 3a) Regulatory potential (RP) scores were used for SNP selection, where an RP score >0.1 indicated the presence of regulatory elements. SNPs without RP scores were also selected. 3b) Prediction of regulatory elements by ChIP-seq data and DNase-seq data. (A) Transcription factor binding sites, (B) histone modification sites (CTCF binding, H3K4me1, H3K4me2, H3K4me3, H3K27ac, H3K9ac), and (C) DNase I hypersensitivity sites were evaluated. ChIP-seq and DNase-seq data derived from GM12878 EBV-transformed B cells were used for *NFKBIE* and *RTKN2*. DNase-seq data of Th1, Th2, and Jurkat cells were also used for *RTKN2*. (Step 4) Association data of the imputation-based GWAS using 1000G reference genotypes were used. SNPs with a significance level of $P<0.05$ were selected. SNPs without association data were also selected. (Step 5) EMSAs and luciferase assays were performed for evaluation of regulatory potentials *in vitro*.
doi:10.1371/journal.pgen.1002949.g004

should be refined as the quality and quantity of genomic databases improves in the future.

We identified multiple candidate causal variants in *NFKBIE* (two nsSNPs and one rSNP) and *RTKN2* (two rSNPs). We could not statistically distinguish the primary effect of each candidate causal variant, because these variants are in strong LD and on the same common haplotype. However, multiple causal variants could be involved in a single locus, which is also seen in another well-known autoimmune locus in 6q23 (*TNFAIP3* gene locus), where both an nsSNP and a regulatory variant have been shown to be functionally related to the disease [8,37]. The risk haplotype of nsSNPs in *NFKBIE* (rs2233433 and rs2233434) showed an enhancement of NF-κB activity, which might reflect an impaired inhibitory effect of IκB-ε on nuclear translocation of NF-κB. On the other hand, down-regulated *NFKBIE* expression and up-regulated *RTKN2* expression were observed at the risk haplotypes, which may be regulated in *cis* by the rSNPs (rs2233424 in *NFKBIE*, rs12248974 and rs61852964 in *RTKN2*). As overexpression studies have also demonstrated dose-dependent attenuation of NF-κB activity by *NFKBIE*, and dose-dependent enhancement by *RTKN2*, the *cis*-regulatory effects of these rSNPs should enhance the NF-κB activity in the risk allele. Taken together with the effect of nsSNPs in *NFKBIE*, the enhancement of NF-κB activity may play a role in the pathogenesis of the disease. This is further supported by evidence that previous GWAS for RA have also identified genes related to the NF-κB pathway, such as *TNFAIP3* [13], v-rel

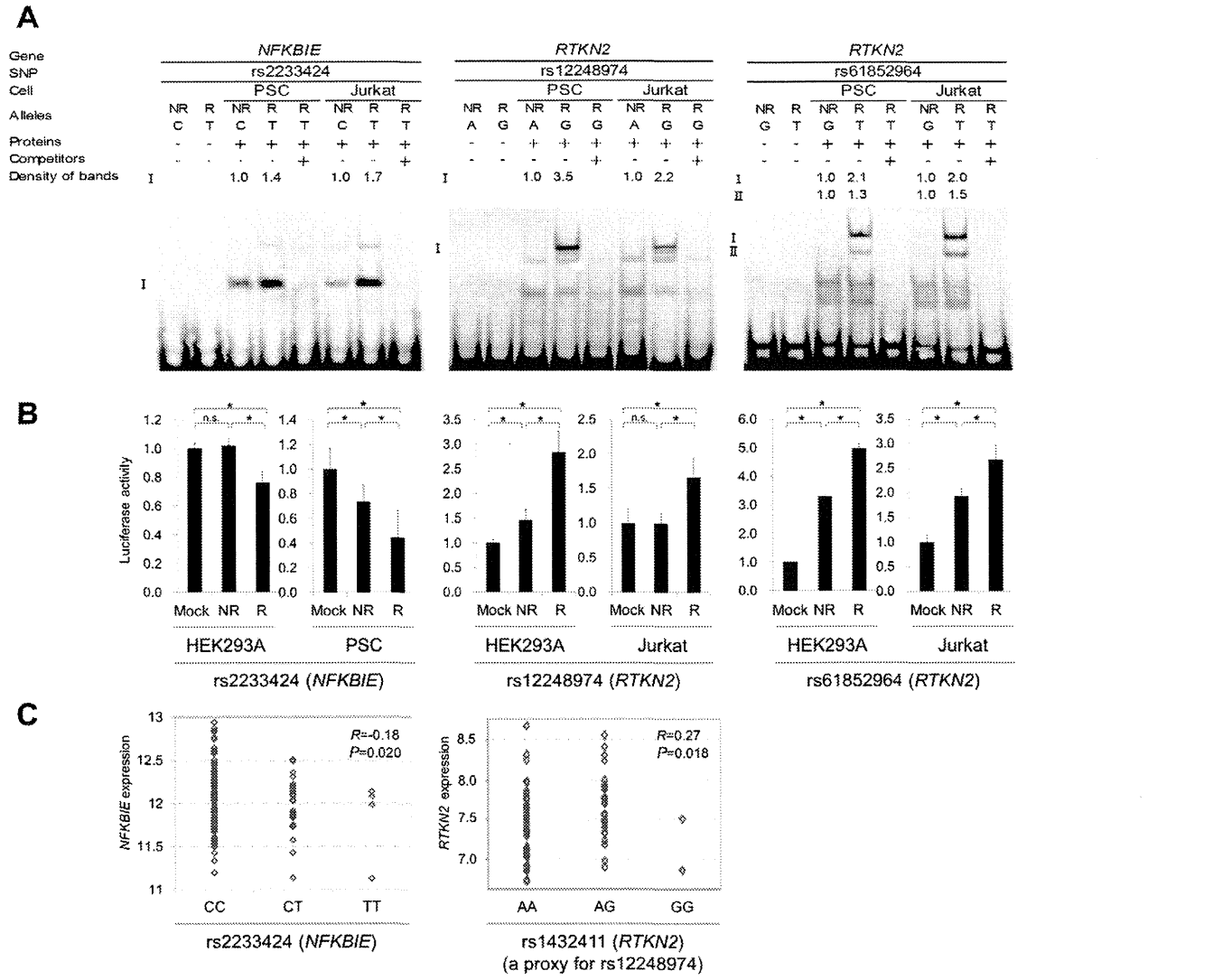

Figure 5. Evaluation of candidate regulatory SNPs *in vitro*. (A) Binding of nuclear factors from lymphoblastoid B-cells (PSC cells) and Jurkat cells to the 31-bp sequences around each SNP was evaluated by EMSA. Unlabeled probes in 200-fold excess as compared to the labeled probes were used for the competition experiment. The densities of the bands were quantified and normalized to that of the risk allele. rs2233424 in *NFKBIE* (C(NR)/T(R)) (left), rs12248974 (A(NR)/G(R)) (middle) and rs61852964 (G(NR)/T(R)) (right) in *RTKN2*. (B) Transcriptional activities were evaluated by luciferase assays. Each 31-bp oligonucleotide was inserted into the pGL4.24[*Luc2P*/minP] vector. Luc, luciferase; minP, minimal promoter. Transcfection was performed with HEK293A (for all the SNPs), PSC cells (for rs2233424), and Jurkat cells (for rs12248974 and rs61852964). rs2233424 (left), rs12248974 (middle), and rs61852964 (right). Data represent the mean ± s.d. Each experiment was performed in sextuplicate and independently repeated three times. *$P<0.05$ by Student's *t*-test. n.s.: not significant. (C) Liner regression analysis of the relationship between SNP genotype and gene expression level. *NFKBIE* expression data in lymphoblastoid B-cell lines of HapMap individuals (JPT+CHB, CEU and YRI; $n=151$), and *RTKN2* expression data in primary T cells from umbilical cords of Western European individuals ($n=85$) were used. The x-axis shows the SNP genotypes and the y-axis represents the $\log_2$-transformed gene expression level. R: correlation coefficient between SNP genotype and gene expression. Rs2233424 genotypes and *NFKBIE* expression level (left). The genotype classification by population: JPT+CHB, CC = 52, CT = 1; CEU, CC = 35, CT = 2; YRI, CC = 32, CT = 2, TT = 4. Rs1432411 genotypes and *RTKN2* expression level (right). Rs1432411 was used as a proxy SNP of rs12248974 ($r^2=0.97$).
doi:10.1371/journal.pgen.1002949.g005

reticuloendotheliosis viral oncogene homolog (*REL* [MIM 164910]) [5], TNF receptor-associated factor 1 (*TRAF1* [MIM 601711]) [3], and CD40 molecule TNF receptor superfamily member 5 (*CD40* [MIM 109535]) [38].

In conclusion, we identified *NFKBIE* and *RTKN2* as genetic risk factors for RA. Considering the allelic effect of both genes, enhanced NF-κB activity may play a role in the pathogenesis of the disease. Because NF-κB regulates the expression of numerous genes, including inflammatory and immune response mediators, NF-κB and its regulators identified by GWAS are promising targets for the treatment of RA.

Materials and Methods

Ethics statement

All subjects were of Japanese origin and provided written informed consent for participation in the study, which was approved by the ethical committees of the institutional review boards.

Subjects

A total of 7,907 RA cases, 657 SLE cases, 1,783 GD cases, and 35,362 control subjects were enrolled in the study through medical

institutes in Japan under the support of the BioBank Japan Project, Center for Genomic Medicine at RIKEN, the University of Tokyo, Tokyo Women's Medical University, and Kyoto University. The same case and control samples were used in the previous meta-analysis of GWASs in the Japanese population (Table S1) [15] . RA and SLE subjects met the revised American College of Rheumatology (ACR) criteria for RA [39]. Diagnosis of individuals with GD was established on the basis of clinical findings and results of the routine examinations for circulating thyroid hormone and thyroid-stimulating hormone concentrations, thyroid-stimulating hormone receptors, ultrasonography, $^{[99m]}TCO_4^-$ (or $[^{123}I]$) uptake, and thyroid scintigraphy. DNAs were extracted from peripheral blood cells using a standard protocol. Total RNAs were also extracted from PBMCs of healthy individuals ($n=20$) using an RNeasy kit (QIAGEN, Valencia, CA, USA). Details of the samples are summarized in Table S1.

Genotyping and quality control

In the GWAS, RA cases and controls were genotyped using Illumina Human610-Quad and Illumina Human 550v3 Genotyping BeadsChips (Illumina, San Diego, CA, USA), respectively, and quality control of genotyping was performed as described previously [6]. For replication study of candidate loci, a landmark SNP was selected from each locus that satisfied $5\times10^{-8}<P_{GWAS}<5\times10^{-5}$ in the GWAS. If multiple candidate SNPs existed within ±100 kb, the SNP with the lowest *P*-value was selected. All case subjects in the replication study and both case and control subjects in the validation study of candidate causal variants were genotyped using TaqMan SNP genotyping assays (Table S12) (Applied Biosystems, Foster City, CA, USA) with an ABI Prism 7900HT Sequence Detection System (Applied Biosystems). Because of the availability of DNA samples, only a part of the control subjects were genotyped for the validation study ($n=3,290$, 97.3%). To enlarge the number of subjects and enhance statistical power for replication studies, we used genotype data obtained from other GWAS projects genotyped using the Illumina platforms for the replication control panels (Table S1). All SNPs were successfully genotyped with call rates >0.98 and were in Hardy-Weinberg equilibrium (HWE) in control subjects ($P>0.05$ as examined by χ^2 test), except for rs2233434, which displayed a deviation from HWE ($P=0.00091$). To evaluate possible genotyping biases between the platforms, we also genotyped rs2233434 and rs3125734 by TaqMan assays for randomly selected subjects genotyped using other genotyping platforms ($n=376$), yielding high concordance rates of ≥0.99.

Association analysis

The associations of the SNPs were tested with the Cochran-Armitage trend test. Combined analysis was performed with the Mantel-Haenszel method. Haplotype association analysis and haplotype-based conditional association analysis were performed using Haploview v4.2 and the PLINK v1.07 program (see URLs) [40], respectively. The SNPs that were not genotyped in the GWAS were imputed using MACH 1.0.16 (see URLs), with genotype data from the 1000 Genome Project (JPT, CHB, and Han Chinese South (CHS): 177 individuals) as references (August 2010 release) [41]. All the imputed SNPs demonstrated *Rsq* values more than 0.60.

DNA re-sequencing

Unknown variants in the coding sequences of *NFKBIE* and *RTKN2* were revealed by directly sequencing the DNA of 48 individuals affected with RA. DNA fragments were amplified with the appropriate primers (Table S13). Purification of PCR products was performed with Exonuclease I (New England Biolabs, Ipswich, MA, USA) and shrimp alkaline phosphatase (Promega, Madison, WI, USA). The amplified DNAs were sequenced using the BigDye Terminator v3.1 Cycle Sequencing kit (Applied Biosystems), and signals were detected using an ABI 3700 DNA Analyzer (Applied Biosystems).

Construction of haplotype-specific expression vectors

The full coding regions were amplified using cDNAs prepared from an Epstein-Barr virus-transfected lymphoblastoid B-cell line (Pharma SNP Consortium (PSC), Osaka, Japan) for *NFKBIE* (NM_004556.2) and from Jurkat cells (American Type Culture Collection (ATCC), Rockville, MD, USA) for *RTKN2* (NM_145307.2) with appropriate primers (Table S14) and DNA polymerases. PCR products were inserted into the pcDNA3.1D/V5-His-TOPO vector (Invitrogen, Camarillo, CA, USA) using the TaKaRa Ligation kit ver. 2.1 (Takara Bio Inc, Shiga, Japan), and mutagenized using the AMAP Multi Site-Directed Mutagenesis Kit (MBL, Nagoya, Japan). Each construct was then transformed into Jet Competent *Escherichia coli* cells (DH5α) (BioDynamics Laboratory Inc., Tokyo, Japan). These plasmids were purified using an Endofree Plasmid Maxi Kit (QIAGEN) after confirmation of the sequence.

NF-κB reporter assay

Human embryonic kidney (HEK) 293A cells (Invitrogen) were cultured in Dulbecco's modified Eagle's medium (Sigma-Aldrich, St. Louis, MO, USA) supplemented with 10% fetal bovine serum (BioWest, Nuaillé, France), 1% penicillin/streptomycin (Invitrogen), and 0.1 mM MEM Non-Essential Amino Acids (Invitrogen). Various doses of the haplotype-specific expression vector (0.0025–0.02 μg for *NFKBIE* and 0.1–0.8 μg for *RTKN2*), pGL4.32[*luc2P*/NF-κB-RE/Hygro] vector (Promega) (0.05 μg and 0.0125 μg, respectively), and pRL-TK vector (an internal control for transfection efficiency) (0.45 μg and 0.15 μg, respectively) were transfected into the HEK293A cells using the Lipofectamine LTX transfection reagent (Invitrogen) according to the manufacturer's protocol. The total amounts of DNAs were adjusted with empty pcDNA3.1 vector. After 22 h, cells were incubated with 1 ng/ml TNF-α (Sigma) for 2 h or with medium alone. Cells were collected, and luciferase activity was measured using a Dual-Luciferase Reporter Assay system (Promega) and a GloMax-Multi+ Detection System (Promega). Each experiment was independently repeated three times, and sextuplicate samples were assayed each time.

Western blotting

After 24 h of transfection as described for the NF-κB reporter assay, cells were lysed in NP-40 lysis buffer (150 mM NaCl, 1% NP-40, 50 mM Tris-HCl at pH 8.0, and a protease inhibitor cocktail), and incubated on ice for 30 min. After centrifugation, the supernatant fraction was collected and 4×Sodium dodecyl sulfate (SDS) sample buffer was added. After denaturation at 95°C for 5 min, proteins were analyzed by SDS-polyachrylamide gel electrophoresis (PAGE) on a 5% to 20% gradient gel (Wako, Osaka, Japan) and were transferred to polyvinylidene difluouride (PVDF) membranes (Millipore, Billerica, MA, USA). Target proteins on the membrane were probed with antibodies (mouse anti-V5 tag (Invitrogen), anti-β-actin-HRP (an internal control), and goat anti-mouse IgG2a-HRP (Santa Cruz Biotechnology, Santa Cruz, CA, USA)), visualized using enhanced chemiluminescence (ECL) detection reagent (GE Healthcare, Pollards Wood, UK), and detected using a LAS-3000 mini lumino-image analyzer

(Fujifilm, Tokyo, Japan). Band intensities were measured using MultiGauge software (Fujifilm).

Allele-specific transcript quantification (ASTQ) analysis

ASTQ analysis was performed as previously described [42]. Total RNAs and genomic DNAs were extracted from PBMCs and lymphoblastoid B-cell lines. cDNAs were synthesized using TaqMan reverse transcription reagents (Applied Biosystems). We selected SNPs (rs2233434 (A/G) for *NFKBIE* and rs3125734 (C/T) for *RTKN2*) as target SNPs. Allele-specific gene expression was measured by TaqMan SNP genotyping probes for these SNPs (Applied Biosystems). To make a standard curve, we selected two individuals that had homozygous genotypes of each target SNP. We mixed these DNAs at nine different ratios and detected the intensities. The $\log_2$ of (risk allele/non-risk allele intensity) for each SNP was plotted against the $\log_2$ of mixing homozygous DNAs. We generated a standard curve (linear regression line; $y = ax+b$), where y is the $\log_2$ of (risk allele/non-risk allele intensity) at a given mixing ratio, x is the $\log_2$ of the mixing ratio, a is the slope, and b is the intercept. We then measured the allelic ratio for each cDNA and genomic DNA from each individual by real-time TaqMan PCR. Based on a standard curve, we calculated the allelic ratio of cDNAs and genomic DNAs. Intensities were detected using an ABI Prism 7900HT Sequence Detection System (Applied Biosystems).

Electrophoretic mobility shift assays (EMSA)

EMSA and preparation of nuclear extract from lymphoblastoid B-cell lines and Jurkat cells were performed as previously described [43]. Cells were cultured in RPMI-1640 medium (Sigma-Aldrich) supplemented with 10% fetal bovine serum and 1% penicillin/streptomycin. Following stimulation with 50 ng/ml phorbol myristate acetate (Sigma-Aldrich) for 2 h, cells were collected and suspended in buffer A (20 mM HEPES at pH 7.6, 20% glycerol, 10 mM NaCl, 1.5 mM $MgCl_2$, 0.2 mM EDTA at pH 8.0, 1 mM DTT, 0.1% NP-40, and a protease inhibitor cocktail) for 10 min on ice. After centrifugation, the pellets were resuspended in buffer B (which contains buffer A with 500 mM NaCl). Following incubation on ice for 30 min and centrifugation to remove cellular debris, the supernatant fraction containing nuclear proteins was collected. Oligonucleotides (31-bp) were designed that corresponded to genomic sequences surrounding the SNPs (Table S15). Single-stranded oligonucleotide probes were labeled using a Biotin 3′ End DNA Labeling Kit (Pierce Biotechnology, Rockford, IL, USA), and sense and antisense oligonucleotides were then annealed. DNA-protein interactions were detected using a LightShift Chemiluminescent EMSA kit (Pierce Biotechnology). The DNA-protein complexes were separated on a non-denaturing 5% polyacrylamide gel in 1×TBE (Tris-borate-EDTA) running buffer for 60 min at 150 V. The DNA-protein complexes were then transferred from the gel onto a nitrocellulose membrane (Ambion, Carlsbad, CA, USA), and were cross-linked to the membrane by exposure to UV light. Signals were detected using a LAS-3000 mini lumino-image analyzer (Fujifilm). Allelic differences were analyzed using MultiGauge software (Fujifilm) by measuring the intensity of the bands.

Luciferase assay

Oligonucleotides (31-bp) were designed as described for the EMSAs (Table S15), and complementary sense and antisense oligonucleotides were annealed. To construct luciferase reporter plasmids, pGL4.24[*luc2P*/minP] vector (Promega) was digested with restriction enzymes (XhoI and BglII) (Takara Bio Inc), and annealed oligonucleotide was ligated into a pGL4.24 vector upstream of the minimal promoter. HEK293A ($n = 2.5\times10^5$), lymphoblastoid B-cell lines ($n = 2.0\times10^6$) and Jurkat ($n = 5.0\times10^5$) cells were transfected with the allele-specific constructs (0.4 μg, 1.8 μg and 2.5 μg, respectively) and the pRL-TK vector (0.1 μg, 0.2 μg and 0.25 μg, respectively) using the Lipofectamine LTX transfection reagent (for HEK293A and Jurkat cells) and Amaxa nucleofector kit (Lonza, Basel, Switzerland) (for lymphoblastoid B-cell lines). Cells were collected, and luciferase activity was measured as described for the NF-κB reporter assay. Each experiment was independently repeated three times and sextuplicate samples were assayed each time.

Correlation analysis between gene expression and genotypes

The expression data in lymphoblastoid B-cell lines derived from HapMap individuals ($n = 210$; JPT, CHB, CEU, and YRI) and in primary T cells from umbilical cords of Western European individuals ($n = 85$) from the database of the Gene Expression Variation (Genevar) project were used. SNP genotypes were obtained from HapMap and 1000 Genome Project databases. The expression levels were regressed with the genotype in a liner model. The statistical significance of regression coefficients was tested using Student's *t*-test.

Statistical analysis

We used χ^2 contingency table tests to evaluate the significance of differences in allele frequency in the case-control subjects. We defined haplotype blocks using the solid spine of LD definition of Haploview v4.2, and estimated haplotype frequency and calculated pairwise LD indices (r^2) between pairs of polymorphisms using the Haploview program. Luciferase assay data and ASTQ analysis data were analyzed by Student's *t*-test.

Web resources

The URLs for data presented herein are as follows:
PLINK, http://pngu.mgh.harvard.edu/~purcekk/plink
MACH, http://www.sph.umich.edu/csg/abecasis/mach/
UCSC Genome Browser, http://genome.ucsc.edu/;
Genevar, http://www.sanger.ac.uk/resources/software/genevar/
HapMap Project, http://www.HapMap.org/
1000 Genome Project, http://www.1000genomes.org
Online Mendelian Inheritance in Man (OMIM), http://www.omim.org/

Supporting Information

Figure S1 NF-kB activity was influenced by nsSNPs in *NFKBIE*. NF-κB activities were evaluated by luciferase assays. Allele specific construct, pGL4.32[*luc2P*/NF-κB-RE] luciferase vector, and pRL-TK vector were transfected into HEK293A cells. Four haplotypes (rs2233434-rs2233433; A-C, G-C, A-T, and G-T) were examined. (rs2233434: A = non-risk (NR), G = risk (R); rs2233433: C = NR, T = R). Twenty-two hours after transfection, cells were stimulated with medium alone (A) or TNF-α (B) for 2 h. Data represent the mean ± s.d. Each experiment was performed in sextuplicate, and experiments were independently repeated three times. $*P<0.05$ and $**P<1.0\times10^{-5}$ by Student's *t*-test. n.s.: not significant.
(TIF)

Figure S2 Allelic imbalance of expression in *NFKBIE*. ASTQ was performed using samples from individuals heterozygous for rs2233434 (G/A) in *NFKBIE*. Genomic DNAs and cDNAs were extracted from lymphoblastoid B cells ($n = 9$). The y-axis shows the $\log_2$ ratio of the transcript amounts in target SNPs (risk allele/non-risk

allele). The top bar of the box-plot represents the maximum value and the lower bar represents the minimum value. The top of box is the third quartile, the bottom of box is the first quartile, and the middle bar is the median value. The circle is an outlier. *$P = 5.3 \times 10^{-4}$ by Student's *t*-test.
(TIF)

Figure S3 SNP selection using *in silico* analysis in the *NFKBIE* region. Step 1: Definition of the target region. *P*-values of the SNPs in the GWAS (top) and genomic structure (middle), and the *D'*-based LD map (bottom). The green diamond shapes represent the -$\log_{10}$ of the Cochran-Armitage trend *P*-values. The dashed line indicates the significance threshold ($P < 1 \times 10^{-3}$). The LD map was drawn based on genotype data of the 1000 Genome Project (JPT, CHB and CHS: 177 samples) using Haploview software v4.2. LD blocks were defined by the solid spine method. The red box (top) represents the target region of the *in silico* analysis (Chr6: 44,336,140-44,394,125). Step 2: Target SNPs were extracted from public databases (HapMap and 1000 Genome Project). SNPs with MAF >0.05 were selected. Step 3: Evaluation of regulatory potential. Step 3a: The regulatory potential (RP) score was calculated for sequences surrounding the SNPs by ESPERR (evolutionary and sequence pattern extraction through reduced representations) method. SNPs with RP score >0.1 were selected. Step 3b: Subsequently, SNPs within the predicted, regulatory genomic elements were selected by using ChIP-seq data of transcription factor binding sites (Txn factor), histone modification sites (CTCF binding, H3K4me1, H3K4me2, H3K4me3, H3K27ac, H3K9ac) or DNase-seq data of DNase I hypersensitivity sites (DNase HS). ChIP-seq data and DNase-seq data used the signals derived from GM12878 EBV-transformed B cells. All these analyses of Steps 2 to 3 were performed by using the UCSC genome browser. Step 4: Evaluation of disease association. Association data of both genotyped (green diamonds) and imputed (black diamonds) SNPs in the GWAS samples were used. Red triangles represent 14 extracted SNPs *in silico*. The dashed line indicates the significance threshold ($P < 0.05$).
(TIF)

Figure S4 SNP selection using *in silico* analysis in the *RTKN2* region. SNP selection in the *RTKN2* region was performed the same as in the case of the *NFKBIE* region as described in Figure S3, except that we used DNase-seq data derived from Th1, Th2, and Jurkat cells in addition to GM12878 EBV-transformed B cells.
(TIF)

Figure S5 Results of EMSAs for candidate regulatory SNPs. Binding affinities of nuclear factors from lymphoblastoid B-cells (PSC cells) and Jurkat cells to the 31-bp sequences around each allele of the candidate regulatory SNPs were evaluated by EMSA. Nuclear factors from PSC cells were used for *NFKBIE*, and Jurkat cells were used for *RTKN2*. 14 SNPs in *NFKBIE* (A) and 10 SNPs in *RTKN2* (B) were tested. NR: non-risk allele; R: risk allele. Arrows indicate bands showing allelic differences in each SNP.
(TIF)

Figure S6 Luciferase assays for regulatory SNPs. Transcriptional activities of the 31-bp genomic sequences around the SNPs were evaluated by luciferase assays. Each oligonucleotide was inserted into the pGL4.24[*luc2P*/minP] vector upstream of the minimal promoter (minP), and allele-specific constructs were transfected into HEK293A cells. Relative luciferase activity is expressed as the ratio of luciferase activity of each allele-specific construct to the luciferase activity of the mock construct. Data represent the mean ± s.d. Each experiment was independently repeated three times, and each sample was measured in sextuplicate. *$P < 1 \times 10^{-3}$ by Student's *t*-test. n.s.: not significant. (A) rs2233434 and rs77986492 in the *NFKBIE* region. (B) rs3864793, rs1864836, rs4979765, and rs4979766 in the *RTKN2* region. NR: non-risk allele; R: risk allele.
(TIF)

Figure S7 The correlation between *NFKBIE* expression and rs2233434 and rs77986492 genotypes. Linear regression analysis of the relationship between SNP genotypes and *NFKBIE* expression. Gene expression data from EBV-transformed lymphoblastoid B cell lines of HapMap individuals (JPT+CHB, CEU, and YRI). (A) rs2233434 ($n = 204$) and (B) rs77986492 ($n = 152$). The genotype classification by population: rs2233434 (JPT+CHB, AA = 61, AG = 28, GG = 1; CEU, AA = 52, AG = 2; YRI, AA = 53, AG = 72) and rs77986492 (JPT+CHB, CC = 52, CT = 24; CEU, CC = 35, CT = 2; YRI, CC = 38, CT = 1). The x-axis shows SNP genotypes and the y-axis represents the $\log_2$-transformed *NFKBIE* expression level. *R*: the correlation coefficient between *NFKBIE* expression and SNP genotype.
(TIF)

Figure S8 The correlation between *RTKN2* expression and rs3852694 genotypes. Linear regression analysis of the relationship between the rs3852694 genotype and *RTKN2* expression. Rs3852694 was used as a proxy SNP of rs1864836 ($r^2 = 1.0$). Gene expression data in primary T cells from umbilical cords of Western European individuals ($n = 85$) were presented by using Genevar software. The x-axis shows the rs3852694 genotypes (AA, AG, GG) and the y-axis represents the $\log_2$-transformed *RTKN2* expression level. *R*: the correlation coefficient between *RTKN2* expression and rs3852694 genotype.
(TIF)

Table S1 Summary of samples.
(DOC)

Table S2 Association results of the GWAS and 1st replication study.
(DOC)

Table S3 Association analysis of *NFKBIE* and *RTKN2* with autoimmune diseases.
(DOC)

Table S4 Association analysis of nsSNPs with RA.
(DOC)

Table S5 Haplotype association study of nsSNPs in *NFKBIE*.
(DOC)

Table S6 Haplotype association study of nsSNPs in *RTKN2*.
(DOC)

Table S7 Predicting the effects of nsSNPs on protein function.
(DOC)

Table S8 Association analysis of candidate rSNPs with RA.
(DOC)

Table S9 Haplotype association study of candidate causal SNPs in *NFKBIE*.
(DOC)

Table S10 Haplotype association study of candidate causal SNPs in *RTKN2*.
(DOC)

Table S11 The conditional haplotype-based association analysis of candidate causal SNPs in *RTKN2*.
(DOC)

Table S12 Probes and Primers used for TaqMan assays.
(DOC)

Table S13 Primers used for DNA re-sequencing.
(DOC)

Table S14 Primers used for construction of expression vectors.
(DOC)

Table S15 Oligonucleotides used for EMSAs and Luciferase assays.
(DOC)

Acknowledgments

We thank K. Kobayashi, M. Kitazato, K. Shimane, and all other members of the Laboratory for Autoimmune Diseases, CGM, RIKEN, for their advice and technical assistance. We also thank the members of BioBank Japan, the Rotary Club of Osaka-Midosuji District 2660 Rotary International, and Dr. Miyatake for supporting sample collection. The replication study of RA was performed under the support of the Genetics and Allied research in Rheumatic diseases Networking (GARNET) consortium.

Author Contributions

Conceived and designed the experiments: K Myouzen, Y Kochi, Y Okada, C Terao, K Ikari, K Ohmura, R Yamada, K Yamamoto. Performed the experiments: K Myouzen, Y Kochi, C Terao, A Suzuki, K Ikari, K Ohmura. Analyzed the data: K Myouzen, Y Kochi, Y Okada, C Terao, T Tsunoda, A Takahashi, R Yamada. Contributed reagents/materials/analysis tools: M Kubo, A Taniguchi, F Matsuda, K Ohmura, S Momohara, T Mimori, H Yamanaka, N Kamatani, Y Nakamura. Wrote the paper: K Myouzen, Y Kochi, Y Okada, C Terao, K Yamamoto.

References

1. Gabriel SE (2001) The epidemiology of rheumatoid arthritis. Rheum Dis Clin North Am 27: 269–281
2. Suzuki A, Yamada R, Chang X, Tokuhiro S, Sawada T, et al. (2003) Functional haplotypes of PADI4, encoding citrullinating enzyme peptidylarginine deiminase 4, are associated with rheumatoid arthritis. Nat Genet 34: 395–402
3. Plenge RM, Seielstad M, Padyukov L, Lee AT, Remmers EF, et al. (2007) TRAF1-C5 as a risk locus for rheumatoid arthritis–a genomewide study. N Engl J Med 357: 1199–1209
4. Wellcome Trust Case Control Consortium (2007) Genome-wide association study of 14,000 cases of seven common diseases and 3,000 shared controls. Nature 447: 661–678
5. Gregersen PK, Amos CI, Lee AT, Lu Y, Remmers EF, et al. (2009) REL, encoding a member of the NF-kappaB family of transcription factors, is a newly defined risk locus for rheumatoid arthritis. Nat Genet 41: 820–823
6. Kochi Y, Okada Y, Suzuki A, Ikari K, Terao C, et al. (2010) A regulatory variant in CCR6 is associated with rheumatoid arthritis susceptibility. Nat Genet 42: 515–519
7. Begovich AB, Carlton VE, Honigberg LA, Schrodi SJ, Chokkalingam AP, et al. (2004) A missense single-nucleotide polymorphism in a gene encoding a protein tyrosine phosphatase (PTPN22) is associated with rheumatoid arthritis. Am J Hum Genet 75: 330–337
8. Adrianto I, Wen F, Templeton A, Wiley G, King JB, et al. (2011) Association of a functional variant downstream of TNFAIP3 with systemic lupus erythematosus. Nat Genet 43: 253–258
9. Thomas PD, Kejariwal A (2004) Coding single-nucleotide polymorphisms associated with complex vs. Mendelian disease: evolutionary evidence for differences in molecular effects. Proc Natl Acad Sci U S A 101: 15398–15403
10. Okada Y, Shimane K, Kochi Y, Tahira T, Suzuki A, et al. (2012) A Genome-Wide Association Study Identified AFF1 as a Susceptibility Locus for Systemic Lupus Eyrthematosus in Japanese. PLoS Genet 8: e1002455. doi:10.1371/journal.pgen.1002455
11. Dubois PC, Trynka G, Franke L, Hunt KA, Romanos J, et al. (2010) Multiple common variants for celiac disease influencing immune gene expression. Nat Genet 42: 295–302
12. 1000 Genomes Project Consortium (2010) A map of human genome variation from population-scale sequencing. Nature 467: 1061–1073
13. Plenge RM, Cotsapas C, Davies L, Price AL, de Bakker PI, et al. (2007) Two independent alleles at 6q23 associated with risk of rheumatoid arthritis. Nat Genet 39: 1477–1482
14. Remmers EF, Plenge RM, Lee AT, Graham RR, Hom G, et al. (2007) STAT4 and the risk of rheumatoid arthritis and systemic lupus erythematosus. N Engl J Med 357: 977–986
15. Okada Y, Terao C, Ikari K, Kochi Y, Ohmura K, et al. (2012) Meta-analysis identifies nine new loci associated with rheumatoid arthritis in the Japanese population. Nat Genet 45: 511–516
16. Li Z, Nabel GJ (1997) A new member of the I kappaB protein family, I kappaB epsilon, inhibits RelA (p65)-mediated NF-kappaB transcription. Mol Cell Biol 17: 6184–6190
17. Whiteside ST, Epinat JC, Rice NR, Israel A (1997) I kappa B epsilon, a novel member of the I kappa B family, controls RelA and cRel NF-kappa B activity. Embo J 16: 1413–1426
18. Collier FM, Gregorio-King CC, Gough TJ, Talbot CD, Walder K, et al. (2004) Identification and characterization of a lymphocytic Rho-GTPase effector: rhotekin-2. Biochem Biophys Res Commun 324: 1360–1369
19. Collier FM, Loving A, Baker A, J., McLeod J, Walder K, et al. (2009) RTKN2 Induces NF-kappaB Dependent Resistance to Intrinsic Apoptosis in HEK cells and Regulates BCL-2 Gene in Human CD4+ Lymphocytes. J Cell Death 2: 9–23
20. Makarov SS (2001) NF-kappa B in rheumatoid arthritis: a pivotal regulator of inflammation, hyperplasia, and tissue destruction. Arthritis Res 3: 200–206
21. Kolbe D, Taylor J, Elnitski L, Eswara P, Li J, et al. (2004) Regulatory potential scores from genome-wide three-way alignments of human, mouse, and rat. Genome Res 14: 700–707
22. Taylor J, Tyekucheva S, King DC, Hardison RC, Miller W, et al. (2006) ESPERR: learning strong and weak signals in genomic sequence alignments to identify functional elements. Genome Res 16: 1596–1604
23. Johnson DS, Mortazavi A, Myers RM, Wold B (2007) Genome-wide mapping of in vivo protein-DNA interactions. Science 316: 1497–1502
24. Valouev A, Johnson DS, Sundquist A, Medina C, Anton E, et al. (2008) Genome-wide analysis of transcription factor binding sites based on ChIP-Seq data. Nat Methods 5: 829–834
25. Mikkelsen TS, Ku M, Jaffe DB, Issac B, Lieberman E, et al. (2007) Genome-wide maps of chromatin state in pluripotent and lineage-committed cells. Nature 448: 553–560
26. Ernst J, Kheradpour P, Mikkelsen TS, Shoresh N, Ward LD, et al. (2011) Mapping and analysis of chromatin state dynamics in nine human cell types. Nature 473: 43–49
27. Sabo PJ, Kuehn MS, Thurman R, Johnson BE, Johnson EM, et al. (2006) Genome-scale mapping of DNase I sensitivity in vivo using tiling DNA microarrays. Nat Methods 3: 511–518
28. Dimas AS, Deutsch S, Stranger BE, Montgomery SB, Borel C, et al. (2009) Common regulatory variation impacts gene expression in a cell type-dependent manner. Science 325: 1246–1250
29. Yang TP, Beazley C, Montgomery SB, Dimas AS, Gutierrez-Arcelus M, et al. (2010) Genevar: a database and Java application for the analysis and visualization of SNP-gene associations in eQTL studies. Bioinformatics 26: 2474–2476
30. Stranger BE, Forrest MS, Dunning M, Ingle CE, Beazley C, et al. (2007) Relative impact of nucleotide and copy number variation on gene expression phenotypes. Science 315: 848–853
31. Stranger BE, Nica AC, Forrest MS, Dimas A, Bird CP, et al. (2007) Population genomics of human gene expression. Nat Genet 39: 1217–1224
32. Stahl EA, Raychaudhuri S, Remmers EF, Xie G, Eyre S, et al. (2010) Genome-wide association study meta-analysis identifies seven new rheumatoid arthritis risk loci. Nat Genet 42: 508–514
33. Chu X, Pan CM, Zhao SX, Liang J, Gao GQ, et al. (2011) A genome-wide association study identifies two new risk loci for Graves' disease. Nat Genet 43: 897–901
34. Trynka G, Hunt KA, Bockett NA, Romanos J, Mistry V, et al. (2011) Dense genotyping identifies and localizes multiple common and rare variant association signals in celiac disease. Nat Genet 43: 1193–1201
35. Li Y, Sidore C, Kang HM, Boehnke M, Abecasis GR (2011) Low-coverage sequencing: implications for design of complex trait association studies. Genome Res 21: 940–951
36. Degner JF, Pai AA, Pique-Regi R, Veyrieras JB, Gaffney DJ, et al. (2012) DNase I sensitivity QTLs are a major determinant of human expression variation. Nature 482: 390–394
37. Musone SL, Taylor KE, Lu TT, Nititham J, Ferreira RC, et al. (2008) Multiple polymorphisms in the TNFAIP3 region are independently associated with systemic lupus erythematosus. Nat Genet 40: 1062–1064
38. Raychaudhuri S, Remmers EF, Lee AT, Hackett R, Guiducci C, et al. (2008) Common variants at CD40 and other loci confer risk of rheumatoid arthritis. Nat Genet 40: 1216–1223
39. Arnett FC, Edworthy SM, Bloch DA, McShane DJ, Fries JF, et al. (1988) The American Rheumatism Association 1987 revised criteria for the classification of rheumatoid arthritis. Arthritis Rheum 31: 315–324
40. Purcell S, Neale B, Todd-Brown K, Thomas L, Ferreira MA, et al. (2007) PLINK: a tool set for whole-genome association and population-based linkage analyses. Am J Hum Genet 81: 559–575
41. Li Y, Willer C, Sanna S, Abecasis G (2009) Genotype imputation. Annu Rev Genomics Hum Genet 10: 387–406